Heliyon 10 (2024) e38122

Contents lists available at ScienceDirect

Heliyon

journal homepage: www.cell.com/heliyon

Research article

Integrative analysis of the efficacy and pharmacological mechanism of Xuefu Zhuyu decoction in idiopathic pulmonary fibrosis via evidence-based medicine, bioinformatics, and experimental verification

Huizhe Zhang [a,1], Haibing Hua [b,1], Jian Liu [c,1], Cong Wang [d,e], Chenjing Zhu [d,e], Qingqing Xia [d,e], Weilong Jiang [d,e], Xiangjin Cheng [f,**], Xiaodong Hu [d,e,***], Yufeng Zhang [d,e,*]

[a] *Department of Respiratory Medicine, Yancheng TCM Hospital Affiliated to Nanjing University of Chinese Medicine, Yancheng TCM Hospital, Yancheng, Jiangsu, 224005, China*
[b] *Department of Gastroenterology, Jiangyin Hospital of Traditional Chinese Medicine, Jiangyin Hospital Affiliated to Nanjing University of Chinese Medicine, Jiangyin, Jiangsu, 214400, China*
[c] *Department of Respiratory Medicine, Xuejia People's Hospital of Xinbei District, Changzhou, Jiangsu, 213003, China*
[d] *Department of Pulmonary and Critical Care Medicine, Jiangyin Hospital of Traditional Chinese Medicine, Jiangyin Hospital Affiliated to Nanjing University of Chinese Medicine, Jiangyin, Jiangsu, 214400, China*
[e] *Research Institute of Respiratory Diseases, Jiangsu Province Clinical Academy of Traditional Chinese Medicine (Jiangyin Branch), Jiangyin, Jiangsu, 214400, China*
[f] *Department of Critical Care Medicine, Yancheng TCM Hospital Affiliated to Nanjing University of Chinese Medicine, Yancheng TCM Hospital, Yancheng, Jiangsu, 224005, China*

A B S T R A C T

Objective: We used evidence-based medicine, bioinformatics and experimental verification to comprehensively analyze the efficacy and pharmacological mechanism of Xuefu Zhuyu decoction (XFZYD) in the treatment of idiopathic pulmonary fibrosis (IPF).
Methods: Major databases were retrieved for randomized controlled trials (RCTs) of XFZYD treating IPF to perform meta-analysis. Active ingredients and target genes of XFZYD were identified from the Traditional Chinese Medicine Systems Pharmacology Database and Analysis Platform (TCMSP). IPF-related differentially expressed genes (DEGs) were identified from the Gene Expression Omnibus (GEO) database. The RGUI software was utilized for Gene Ontology (GO) functional enrichment and Kyoto Encyclopedia of Genes and Genomes (KEGG) pathway enrichment analyses. The ingredient-target and protein-protein interaction (PPI) networks were achieved through Cytoscape software and the STRING database to identify the key compounds and target proteins. Molecular docking was performed using AutoDockTool and AutoDock Vina software. The effect between key compounds and target proteins was verified in animal experiments.

* Corresponding author. Department of Pulmonary and Critical Care Medicine, Jiangyin Hospital of Traditional Chinese Medicine, Jiangyin Hospital Affiliated to Nanjing University of Chinese Medicine, Jiangyin, Jiangsu, 214400, China.
** Corresponding author. Department of Critical Care Medicine, Yancheng TCM Hospital Affiliated to Nanjing University of Chinese Medicine, Yancheng TCM Hospital, Yancheng, Jiangsu, 224005, China.
*** Corresponding author. Department of Pulmonary and Critical Care Medicine, Jiangyin Hospital of Traditional Chinese Medicine, Jiangyin Hospital Affiliated to Nanjing University of Chinese Medicine, Jiangyin, Jiangsu, 214400, China.
E-mail addresses: 20195145@njucm.edu.cn (H. Zhang), hhbjytcm@163.com (H. Hua), ss8738@163.com (J. Liu), sushi345@163.com (C. Wang), 532964377@qq.com (C. Zhu), xqqjytcm@163.com (Q. Xia), jwljytcm@163.com (W. Jiang), 13861419668@163.com (X. Cheng), huxido2000@sina.com (X. Hu), yufengzhang@njucm.edu.cn (Y. Zhang).
[1] Huizhe Zhang, Haibing Hua and Jian Liu contributed to the work equally and should be regarded as co-first authors.

https://doi.org/10.1016/j.heliyon.2024.e38122
Received 11 February 2024; Received in revised form 16 September 2024; Accepted 18 September 2024
Available online 20 September 2024

Results: Six RCTs were included for meta-analysis, which uncovered that the total effective rate of clinical efficacy was higher in the experimental group than control group. Then, 156 active ingredients and 254 target genes of XFZYD, and 1,566 IPF-related DEGs were identified. The intersection analysis identified 48 target genes correlating with 130 active ingredients of XFZYD treating IPF. GO functional enrichment, KEGG pathway enrichment, ingredient-target network and PPI network were achieved. Following the identification of key compounds and target proteins, we performed molecular docking. Ultimately, our research focused on the key compound quercetin for experimental validation to assess its interactions with two key target proteins, JUN and PTGS2.
Conclusion: The effectiveness of XFZYD on IPF has been substantiated through evidence-based medicine. The pharmacological mechanism of XFZYD for IPF treatment involves a complex interplay of various compounds and targets, with quercetin exerting pronounced impacts on JUN and PTGS2 proteins.

1. Introduction

Idiopathic pulmonary fibrosis (IPF) represents a distinct subtype of progressive fibrosing interstitial lung disease characterized by escalating severity of dyspnea, restrictive ventilatory impairment, disturbances in gas exchange, development of hypoxemia, and a heightened risk of respiratory failure [1,2]. The diagnostic imaging of IPF using chest high-resolution computed tomography (HRCT) or lung histological examination frequently reveals manifestation of usual interstitial pneumonia (UIP) [3]. IPF is a relatively rare condition predominantly affecting the aging population. The current incidence rates in North American and European populations range from 2.8 to 9.3 cases per 100,000 individuals. Despite limited epidemiological data on this condition in China, a substantial and rapid rise has been noted in the prevalence of IPF over the last decade [4,5].

Currently, IPF is widely considered incurable. In clinical settings, the primary therapeutic goals are to mitigate the deterioration of lung functions, facilitate the quality of life (QOL) for patients, and curb further disease progression. Western medications, particularly pirfenidone and nintedanib, have exhibited promising effectiveness in treating IPF. Nevertheless, their patient accessibility is constrained due to substantial costs and the risk of adverse reactions [6]. The significance of traditional Chinese medicine (TCM) in treating IPF has gained growing recognition in recent years. Clinical trials and meta-analyses have demonstrated that herbal medicine for IPF treatment can alleviate disease symptoms, decelerate the decline of lung functions, and enhance the overall QOL for patients [7,8]. Furthermore, research reports have substantiated that herbal medicine positively affects lung histopathology and physiological indicators of bleomycin-induced animal models [9,10].

Xuefu Zhuyu decoction (XFZYD), initially introduced during the Qing Dynasty, is a widely used TCM remedy to modulate qi and stimulate blood circulation. It is composed of *Semen Persicae* (SP, Taoren), *Flos Carthami* (FC, Honghua), *Radix Paeoniae Rubra* (RPR, Chishao), *Rhizoma Chuanxiong* (RC, Chuanxiong), *Radix Achyranthis Bidentatae* (RAB, Niuxi), *Radix Angelicae Sinensis* (RAS, Danggui), *Radix Rehmanniae* (RR, Shengdihuang), *Radix Platycodi* (RP, Jiegeng), *Fructus Aurantii* (FA, Zhike), *Radix Bupleuri* (RB, Chaihu) and *Radix Glycyrrhizae* (RG, Gancao) [11,12]. In accordance with the principles of TCM, SP and FC are 'monarch herbs' in XFZYD, serving as the principal components of XFZYD.

XFZYD, when administered orally, functions to augment blood circulation and eliminate blood stasis, concurrently facilitating qi circulation and pain relief. Clinical investigations have demonstrated substantial therapeutic benefits of XFZYD in the treatment of IPF [13,14]. Moreover, preliminary findings from animal studies have indicated the capability of XFZYD to diminish the severity of pulmonary fibrosis (PF) in rats, thereby underscoring its potential in PF treatment [15,16]. A prior meta-analysis has unveiled that the incorporation of XFZYD into conventional western medicine treatment contributes to enhanced clinical efficacy and improved lung functions among patients suffering from PF, including those with fibrosis following radiotherapy for lung cancer [17]. Nevertheless, the therapeutic efficacy and pharmacological basis of XFZYD in IPF are not well-characterized. There is a pressing concern to advance the evidence-based clinical application of XFZYD, clarify its clinical efficacy, explore the mechanistic underpinnings, and optimize its formulation. Therefore, it is crucial to establish clinical efficacy through evidence-based medicine and to further examine the pharmacological impact of XFZYD on IPF.

In the present research, we assessed the effectiveness and pharmacological basis of XFZYD in treating IPF through evidence-based medicine, bioinformatics, and experimental validation. Specifically, the randomized controlled trials (RCTs) focusing on the therapeutic effectiveness of XFZYD in patients with IPF were retrieved for meta-analyses to corroborate the clinical effectiveness of XFZYD. The TCM Systems Pharmacology Database and Analysis Platform (TCMSP), in conjunction with IPF-associated differentially expressed genes (DEGs) from the Gene Expression Omnibus (GEO) database, were utilized to pinpoint target genes of XFZYD for IPF management, followed by functional enrichment analysis via Gene Ontology (GO) and pathway enrichment analysis using Kyoto Encyclopedia of Genes and Genomes (KEGG). Notably, the establishment of ingredient-target and protein-protein interaction (PPI) networks facilitated the selection of key active ingredients and target proteins. Eventually, molecular docking and experimental verification were applied to delineate potential effects between the identified key active ingredients and target proteins.

2. Results

2.1. Systematic review of RCTs in evaluating the clinical efficacy of XFZYD for IPF treatment

In this comprehensive review, we initially identified 79 articles via database search, eventually narrowing them down to 31 articles after eliminating duplicates. The subsequent screening process, involving the review of titles and abstracts, resulted in the selection of

10 articles based on our inclusion criteria for screening studies. Following examination of the full text, six RCTs [13,14,18–21] were included for subsequent analyses. Supplementary Figure S1 shows the literature searching process.

The six selected RCTs [13,14,18–21], all conducted in China, collectively enrolled a total of 714 patients and were characterized by a single-center study design. The primary characteristics of these studies are summarized in Supplementary Table S1.

Methodological quality assessments revealed that three RCTs [14,18,21] utilized a table of random numbers to generate sequences, and no allocation concealment was used across all RCTs. Of note, blinding was not mentioned in any RCTs, though complete outcome data were available for all RCTs. The feasibility of determining selective reporting was not established (Supplementary Table S2, Supplementary Figure S2-S3).

In terms of clinical efficacy, five RCTs [13,14,19–21] evaluated the total effective rate (TER). Regarding lung function, two RCTs [19,20] compared the force vital capacity (FVC); four RCTs [13,14,18,21] examined the FVC% predicted (FVC%); four RCTs [13,14, 18,21] evaluated the forced expiratory volume in 1 s (FEV1); two RCTs [13,19] assessed the FEV1% predicted (FEV1%); two RCTs [14, 21] measured the FEV1/FVC ratio; one RCT [19] analyzed the peak expiratory flow (PEF); one RCT [18] compared PEF% predicted (PEF%); one RCT [20] focused on diffusing capacity of the lung for carbon monoxide (DLCO)% predicted (DLCO%). Adverse reactions to the treatment were reported in three studies [19–21], while the remaining studies [13,14,18] did not mention them (Supplementary Table S3).

2.2. Meta-analyses of clinical effectiveness, lung function, and adverse reactions

The clinical effectiveness was assessed by quantifying TER in five RCTs [13,14,19–21], which collectively involved 390 patients. These studies partitioned the participants into the experimental group (n = 197) and the control group (n = 193). A homogeneity test across these studies revealed consistent results ($Chi^2 = 1.77$, $P = 0.78$, $I^2 = 0$ %). The pooled odds ratio (OR), calculated using a fixed effect model, was 3.25 with a 95 % confidence interval (CI) ranging from 1.89 to 5.59 ($P < 0.0001$), indicating a higher TER and facilitated clinical efficacy in the experiment group compared to the control group (Fig. 1).

Moreover, the meta-analysis results suggested a marked improvement in lung function parameters, such as FVC%, FEV1, FEV1%, and the FEV1/FVC ratio in the experimental group relative to the control group (Supplementary Figure S4). In addition, the meta-analysis of adverse reactions revealed no pronounced differences in the occurrence of adverse effects between the two groups (Supplementary Figure S5).

2.3. Identification of active ingredients and target genes of XFZYD

The screening process using TCMSP yielded 66 active ingredients from SP, 189 from FC, 119 from RPR, 189 from RC, 176 from RAB, 125 from RAS, 76 from RR, 102 from RP, 17 from FA, 349 from RB, and 280 from RG. Based on the criteria of drug-likeness (DL) ≥ 0.18 and oral bioavailability (OB) ≥ 30 % for screening, the number of the selected active ingredients was 23 from SP, 22 from FC, 29 from RPR, 7 from RC, 20 from RAB, 2 from RAS, 2 from RR, 7 from RP, 5 from FA, 17 from RB, and 92 from RG (Supplementary File 1). After eliminating duplications, a list of 197 candidate active ingredients in XFZYD were identified, as detailed in Supplementary Table S4.

In addition, the TCMSP was utilized for the identification of target genes for each of the 197 candidate active ingredients, with 39 active ingredients lacking corresponding target genes. Further refinement from the Universal Protein Resource (UniProt) led to the exclusion of two ingredients without matching gene symbols (Supplementary File 2). Eventually, 254 target genes were pinpointed for the remaining 156 active ingredients in XFZYD (Supplementary Table S5).

2.4. Retrieval and analysis of microarray datasets for IPF-related target genes

Subsequently, we incorporated four microarray datasets, namely GSE2052, GSE21369, GSE24206, and GSE53845, that conformed to our selection criteria to analyze gene expression in IPF. These datasets provided gene expression profiles from IPF and normal

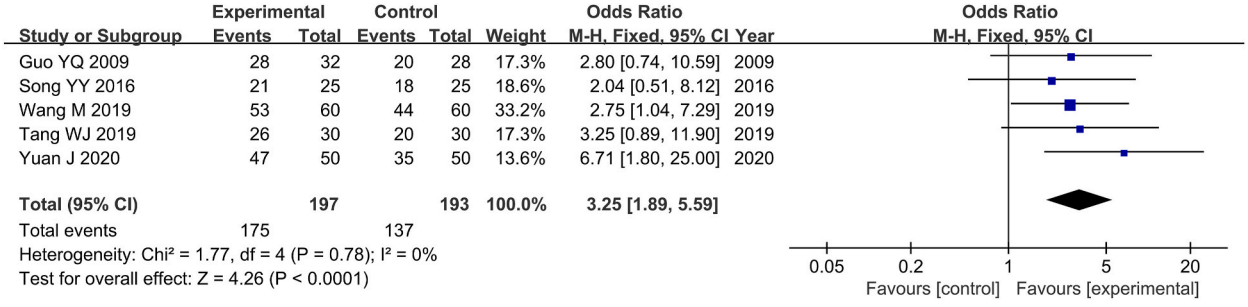

Fig. 1. Comparative forest plot of TER.
The TER for clinical effectiveness demonstrated a prominent elevation in the experimental group compared to the control group (OR = 3.25, 95 % CI 1.89–5.59, $P < 0.0001$).

samples, with GSE2052 utilizing the GPL1739 platform [22–24], GSE21369 and GSE24206 using the GPL570 platform [25,26], and GSE53845 using the GPL6480 platform [27].

Based on the four microarray datasets, different genes identified using GEO2R online tool of each microarray dataset was shown in Supplementary File 3. The identification of DEGs between IPF and normal samples was carried out utilizing the GEO2R, with criteria set at adjusted (adj) $P < 0.05$ and $|\log2FoldChange\ (FC)| > 1$. The resulting DEGs were illustrated through volcano plots (Fig. 2A–D). The integration and deduplication resulted in 1,566 DEGs, which were identified as IPF-associated target genes (Supplementary Table S6).

2.5. Identification of target genes of XFZYD for IPF management

Next, we conducted an intersection analysis between the 254 target genes of XFZYD and the 1,566 IPF-related target genes. This comparison yielded 48 intersecting genes, which were recognized as target genes of XFZYD for IPF management (**Fig. 3**, **Table 1**).

2.6. Analyses of GO functional enrichment

Our examination of the GO biological process (BP) functional enrichment revealed significant involvement of the target genes of XFZYD for IPF management in several BPs, including response to nutrient, response to nutrient levels, regulation of body fluid levels, response to extracellular stimulus, extracellular matrix (ECM) organization, vasoconstriction, response to oxidative stress, extracellular structure organization, negative regulation of blood vessel diameter, and cellular response to oxidative stress (Supplementary File

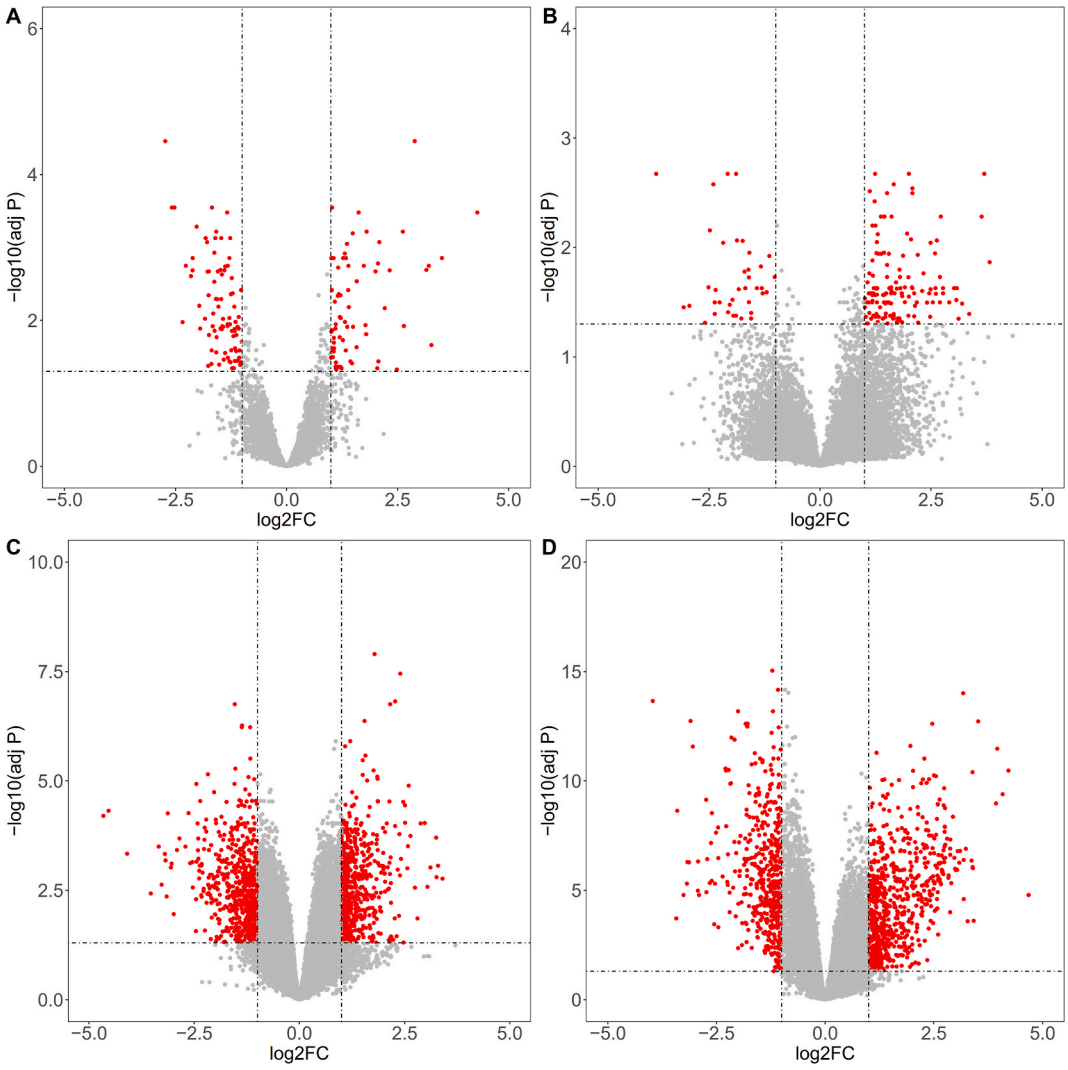

Fig. 2. Identification of DEGs between IPF and normal samples.
The DEGs were pinpointed from the GSE2052 dataset (A), GSE21369 dataset (B), GSE24206 dataset (C), and GSE53845 dataset (**D**).

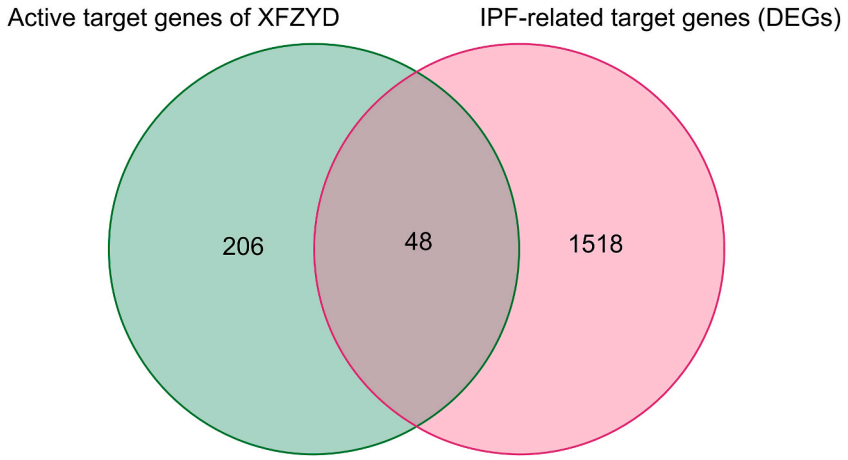

Fig. 3. Target genes of XFZYD for IPF management.
The 254 XFZYD-associated target genes were intersected with the 1,566 IPF-related target genes, leading to the identification of 48 target genes of XFZYD for IPF management.

Table 1
Gene symbol and entrezID of target genes.

Gene symbol	EntrezID	Gene symbol	EntrezID	Gene symbol	EntrezID
PTGS2	5743	AKR1C3	8644	SPP1	6696
ADRA2A	150	MMP3	4314	CTSD	1509
PLAU	5328	CCND1	595	IRF1	3659
MAOA	4128	TOP1	7150	GSTA1	2938
CHRM3	1131	HIF1A	3091	GSTA2	2939
ADRB1	153	CAV1	857	FOSL2	2355
ADRA1A	148	MYC	4609	CYCS	54205
ADRA1B	147	CCL2	6347	SLC6A4	6532
CCNA2	890	CXCL8	3576	FASN	2194
JUN	3725	SERPINE1	5054	LDLR	3949
MMP1	4312	COL1A1	1277	ADIPOR2	79602
CYP3A4	1576	TOP2A	7153	CA2	760
SELE	6401	NQO1	1728	MMP10	4319
VCAM1	7412	COL3A1	1281	MCL1	4170
CYP1B1	1545	CXCL2	2920	CD163	9332
HAS2	3037	CXCL10	3627	EPHB2	2048

4A). The top 20 enriched BPs, determined by adj P values, are visually presented in Fig. 4A.

Our analysis of GO cellular component (CC) functional enrichment for XFZYD target genes in IPF management highlighted prominent enrichment in membrane raft, plasma membrane raft, integral component of presynaptic membrane, membrane microdomain, membrane region, caveola, intrinsic component of presynaptic membrane, ECM, integral component of postsynaptic membrane, and intrinsic component of postsynaptic membrane (Supplementary File 4B). Fig. 4B depicts the top 20 enriched CCs, which were determined by the adj P values.

The results from GO molecular function (MF) functional enrichment for XFZYD target genes in managing IPF demonstrated significant enrichment in protease binding, G protein-coupled amine receptor activity, CXCR chemokine receptor binding, protein heterodimerization activity, heme binding, chemokine receptor binding, tetrapyrrole binding, G protein-coupled receptor binding, platelet-derived growth factor binding, and oxidoreductase activity/acting on the CH-NH2 group of donors/oxygen as acceptor (Supplementary File 4C). The top 20 enriched MFs, determined by adj P values, are illustrated in Fig. 4C.

2.7. Analysis of KEGG pathway enrichment

The KEGG pathway enrichment revealed that XFZYD-associated target genes in IPF management were notably enriched in various pathways, such as tumor necrosis factor (TNF) signaling pathway, interleukin 17 (IL-17) signaling pathway, rheumatoid arthritis, lipid and atherosclerosis, chemical carcinogenesis-receptor activation, fluid shear stress and atherosclerosis, Kaposi sarcoma-associated herpesvirus infection, advanced glycation end products (AGE)-receptor for AGE (RAGE) signaling pathway in diabetes complications, chemical carcinogenesis-DNA adducts, and bladder cancer (Supplementary File 5). Fig. 5 displays the topmost 20 KEGG pathway enrichment as determined by the adj P values.

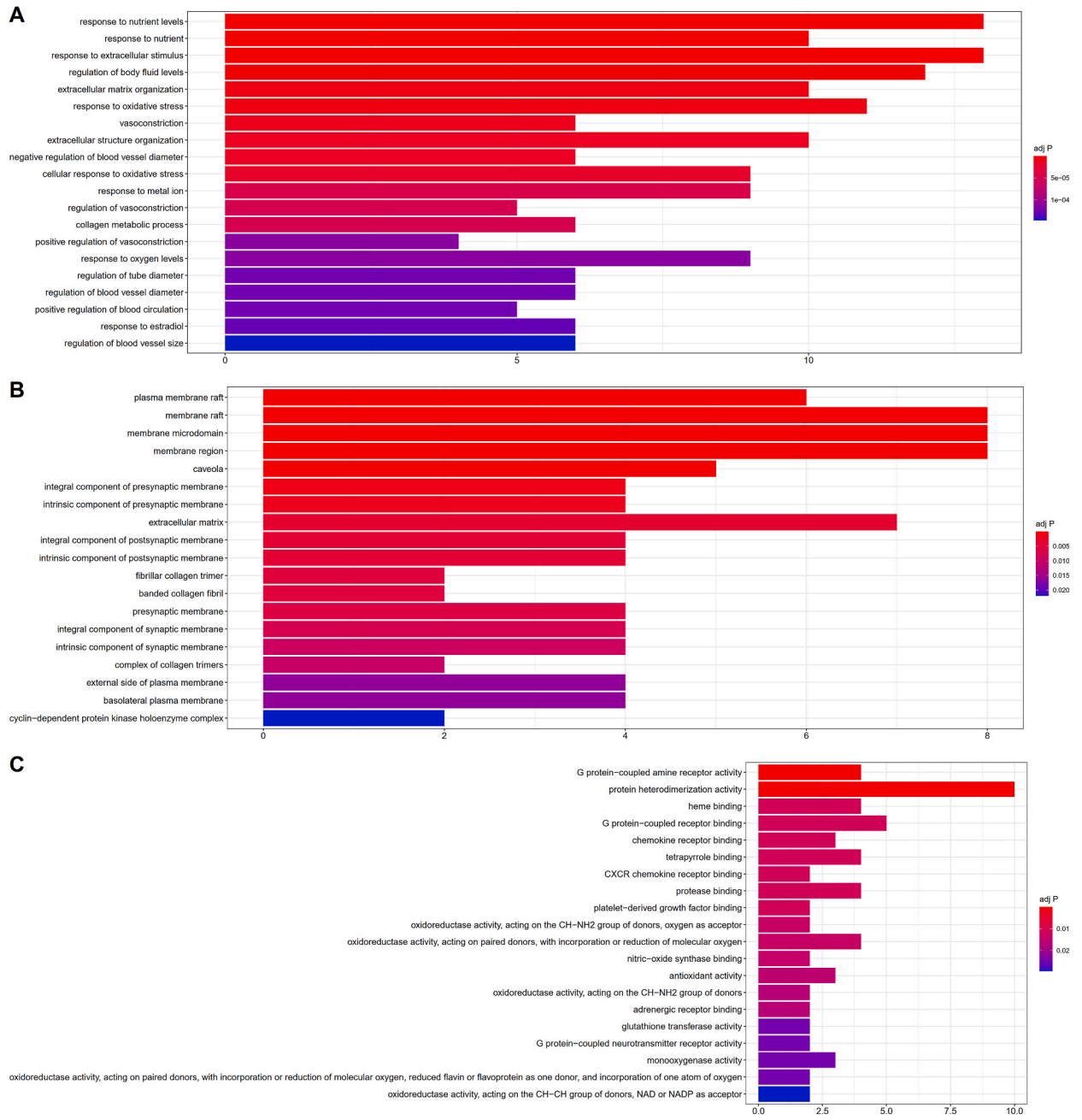

Fig. 4. GO functional enrichment.
GO functional enrichment analyses of BPs (**A**), CCs (**B**), and MFs (**C**) enriched by target genes of XFZYD for IPF management.

2.8. Construction of ingredient-target and PPI networks

The Cytoscape software and its NetworkAnalyzer tool were employed to delineate the connections of the ingredient-target network. In view of the lack of correlation between certain active ingredients and interlacing target genes, we focused on 48 intersecting target genes correlated with 130 active ingredients. The resulting network comprised 178 nodes (130 nodes representing active ingredients and 48 nodes representing target genes) connected by 313 edges (Fig. 6A, Supplementary File 6A). The NetworkAnalyzer tool was further utilized to assess the significance of each active compound based on their degree values in the network. Table 2 summarizes the essential data on the top eight significant compounds, ranked by degree, which were identified as the key active ingredients of XFZYD for IPF management.

The construction of the PPI network was carried out by integrating the 48 corresponding target genes into the STRING database.

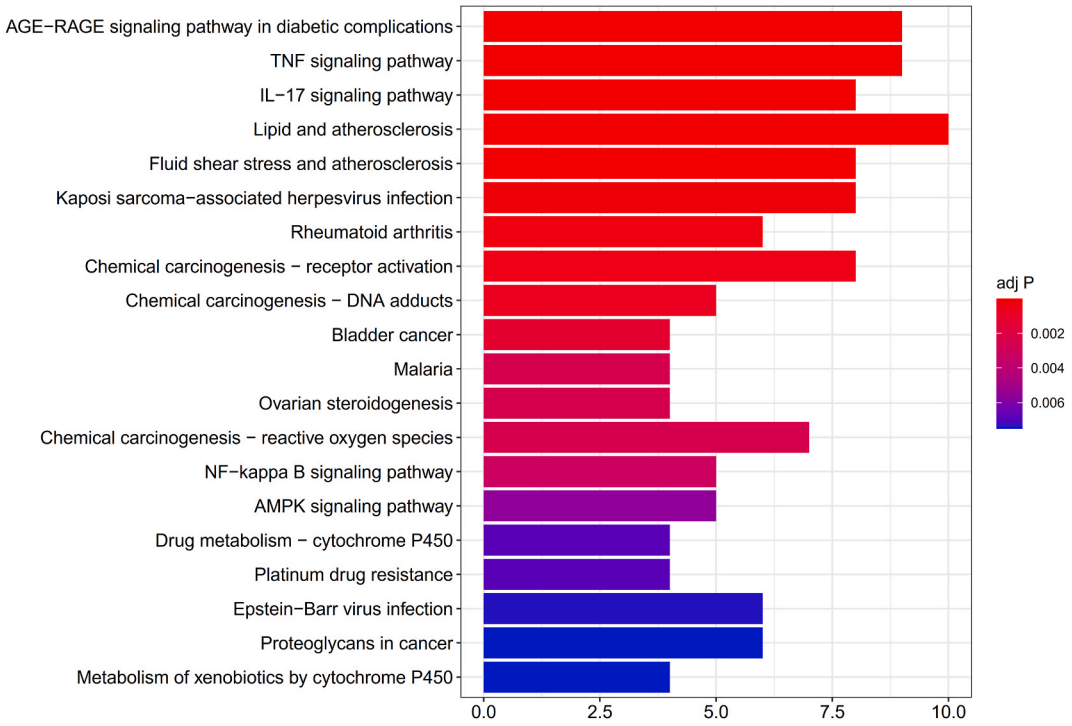

Fig. 5. KEGG pathway enrichment.
The top 20 enriched KEGG pathways for XFZYD target genes in IPF ranked by the adj P values.

With the interaction threshold set at 0.40, the network exhibited interconnectivity among 46 target proteins, resulting in a complex network with 250 edges indicative of PPIs (Fig. 6B–Supplementary File 6B). As indicated in Table 3, the top 10 target proteins in this PPI network, ranked by degree, were considered key target proteins of XFZYD for IPF management.

2.9. Verification of molecular docking interactions

Three-dimensional structural models for the active ingredients and target proteins were sourced from the PubChem and RCSB PDB databases. Subsequently, we conducted molecular docking simulations to ascertain potential interactions between target proteins and their associated active ingredients utilizing the AutoDock Vina and AutoDockTool software. As a representative display, the most significant active ingredient in the network, quercetin, underwent molecular docking with the top two target proteins transcription factor Jun (JUN) and prostaglandin G/H synthase 2 (PTGS2/COX2). The docking of JUN with quercetin yielded a minimum binding affinity of −8.6 kcal/mol, with a grid center positioned at −23.326, 17.311, and 20.955, and a distance from best mode showing an rmsd of 0.000 in both l.b. and u.b. (Fig. 7A–7D). The docking between PTGS2 and quercetin demonstrated a minimum binding affinity of −9.9 kcal/mol, a grid center of 24.338, 41.997, and 39.106, and an rmsd of 0.000 in both l.b. and u.b. (Fig. 7E–7H).

2.10. Assessment of bleomycin-induced IPF model

To evaluate the pathological changes, hematoxylin-eosin (HE) staining was utilized across different study groups. The model group exhibited prominent ECM hyperplasia and alveolar structure impairment after 21 days. Conversely, the XFZYD and quercetin-treated groups displayed relatively preserved alveolar structures and lessened pulmonary interstitial hyperplasia. The severity of PF was further quantified using Masson staining, revealing a pronounced presence of blue-stained collagen fibers in the lung interstitium of the model group after 21 days. In contrast, XFZYD and quercetin-treated groups showed only a mild degree of PF (Fig. 8A). The Szapiel score was significantly higher in the model group, whereas the XFZYD and quercetin-treated groups were improved (Fig. 8B). The Ashcroft score was significantly higher in the model group, whereas the XFZYD and quercetin-treated groups were improved (Fig. 8C). Additionally, the hydroxyproline (HYP) content of model group was remarkably higher than the control group, XFZYD and quercetin exhibited decreases in the HYP contents compared with model group (Fig. 8D). These data indicated the efficacy of XFZYD and quercetin in restoring alveolar structure and reducing PF in a bleomycin-induced IPF model.

2.11. Immunohistochemical assay of the expression of JUN and PTGS2

To further reveal pharmacological mechanism in bleomycin-induced IPF, immunohistochemistry was used to investigate the

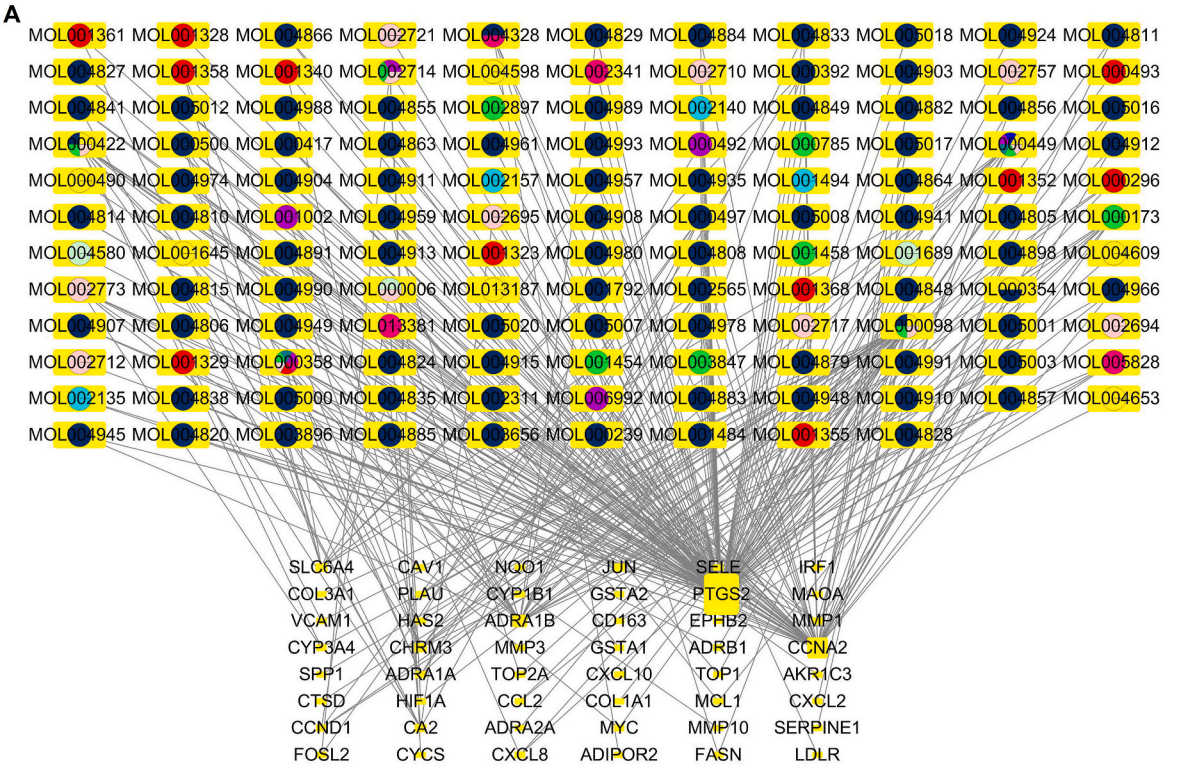

(caption on next page)

Fig. 6. Visualization of ingredient-target and PPI networks.
(**A**) The ingredient-target network comprises 178 nodes (130 nodes representing active ingredients and 48 representing target genes), connected by 313 edges. Active ingredients are depicted as circles with varying color coding for each active ingredient, while target genes are represented as rectangles. The edges in this network illustrate the connections between these nodes. (**B**) The PPI network illustrates interactions among 46 target proteins, with 250 edges symbolizing the PPIs, based on the lowest interaction score of 0.40.

Table 2
Key compounds in XFZYD for IPF management.

Compound name	Compound ID	PubChem CID	Molecular Formula	Degree	Herb
quercetin	MOL000098	5280343	$C_{15}H_{10}O_7$	27	FC, RAB, RB, RG
kaempferol	MOL000422	5280863	$C_{15}H_{10}O_6$	10	FC, RAB, RB, RG
stigmasterol	MOL000449	5280794	$C_{29}H_{48}O$	8	FC, RPR, RAB, RAS, RR, RB
beta-carotene	MOL002773	5280489	$C_{40}H_{56}$	7	FC
luteolin	MOL000006	5280445	$C_{15}H_{10}O_6$	7	FC, RP
wogonin	MOL000173	5281703	$C_{16}H_{12}O_5$	7	RAB
beta-sitosterol	MOL000358	222284	$C_{29}H_{50}O$	6	SP, FC, RPR, RAB, RAS, FA
medicarpin	MOL002565	336327	$C_{16}H_{14}O_4$	6	RG

Table 3
Key target proteins of XFZYD for IPF management.

Key target	Entry	Entry name	Protein name	Degree
JUN	P05412	JUN_HUMAN	Transcription factor Jun	29
PTGS2	P35354	PGH2_HUMAN	Prostaglandin G/H synthase 2	26
CCL2	P13500	CCL2_HUMAN	C-C motif chemokine 2	24
HIF1A	Q16665	HIF1A_HUMAN	Hypoxia-inducible factor 1-alpha	24
MYC	P01106	MYC_HUMAN	Myc proto-oncogene protein	22
CXCL8	P10145	IL8_HUMAN	Interleukin-8	21
SERPINE1	P05121	PAI1_HUMAN	Plasminogen activator inhibitor 1	20
CCND1	P24385	CCND1_HUMAN	G1/S-specific cyclin-D1	20
VCAM1	P19320	VCAM1_HUMAN	Vascular cell adhesion protein 1	20
MMP3	P08254	MMP3_HUMAN	Stromelysin-1	20

expression of JUN and PTGS2 proteins. Bleomycin intervention reduced the expression of these proteins in the model group compared to the control group. In contrast, both XFZYD and quercetin treatment groups exhibited a pronounced elevation in JUN and PTGS2 protein levels (Fig. 9), indicating their potential modulatory impact on bleomycin-induced IPF.

3. Discussion

IPF, a chronic, progressive interstitial lung condition, is histologically characterized by UIP [1,2]. At present, the definitive cure for IPF remains elusive. The therapeutic aim for IPF is to decelerate its progression, augment patient QOL, and enhance survival prospects. The prognosis of IPF is notably bleak, with a median survival time of about 2–3 years following diagnosis [4,5]. Key clinical symptoms, such as cough, dyspnea, and lung function deterioration, are closely linked to the prognosis and independently serve as risk variables for mortality in IPF [28,29].

TCM has increasingly become a prominent approach in managing IPF in recent years [7,8]. According to TCM principles, IPF has been categorized as "*feibi*" (pulmonary arthralgia) and "*feiwei*" (pulmonary fistula), reflecting the symptoms of cough, sputum production, worsening dyspnea, and recurring symptoms. The concept of "*feibi*" originated in the ancient text "*Inner Canon of Huangdi*," whereas "*feiwei*" was first mentioned in Zhang Zhongjing's "*Jinkui Yaolue*." The treatment for these conditions in TCM predominantly involves strategies to nourish the blood and qi [5,30].

XFZYD, known for its ability to enhance blood circulation and modulate qi, comprises a blend of SP, FC, RPR, RC, RAB, RAS, RR, RP, FA, RB, and RG. Of note, SP and FC, as the "monarch herbs," have been suggested to augment blood circulation and diminish blood stasis. RPR and RC contribute to improving blood circulation and relieving blood stasis, while RAB activates blood and ensures its proper downward flow. RAS and RR are key in replenishing qi and blood. RP and FA are effective in promoting qi circulation, RB aids in dispersing stagnant qi, and RG rejuvenates qi and coordinates the overall herbal action [31,32]. The therapeutic approach of XFZYD aligns with the TCM theory for treating IPF, offering symptom alleviation and presenting a potent TCM formulation for addressing "*feibi*" and "*feiwei*" conditions.

Prior clinical studies have demonstrated the substantial therapeutic benefits of XFZYD in treating IPF. There is no systematic review and meta-analysis of XFZYD in the treatment of IPF. A key focus in current research is enhancing the evidence-based application of XFZYD, elucidating its clinical efficacy, and understanding its mechanistic underpinnings to refine its formulation. In the present research, we confirmed the effectiveness of XFZYD in the treatment of IPF through evidence-based medicine and a meta-analysis of six RCTs focusing on this issue. The meta-analysis data showed a markedly higher TER of clinical effectiveness in the experimental group

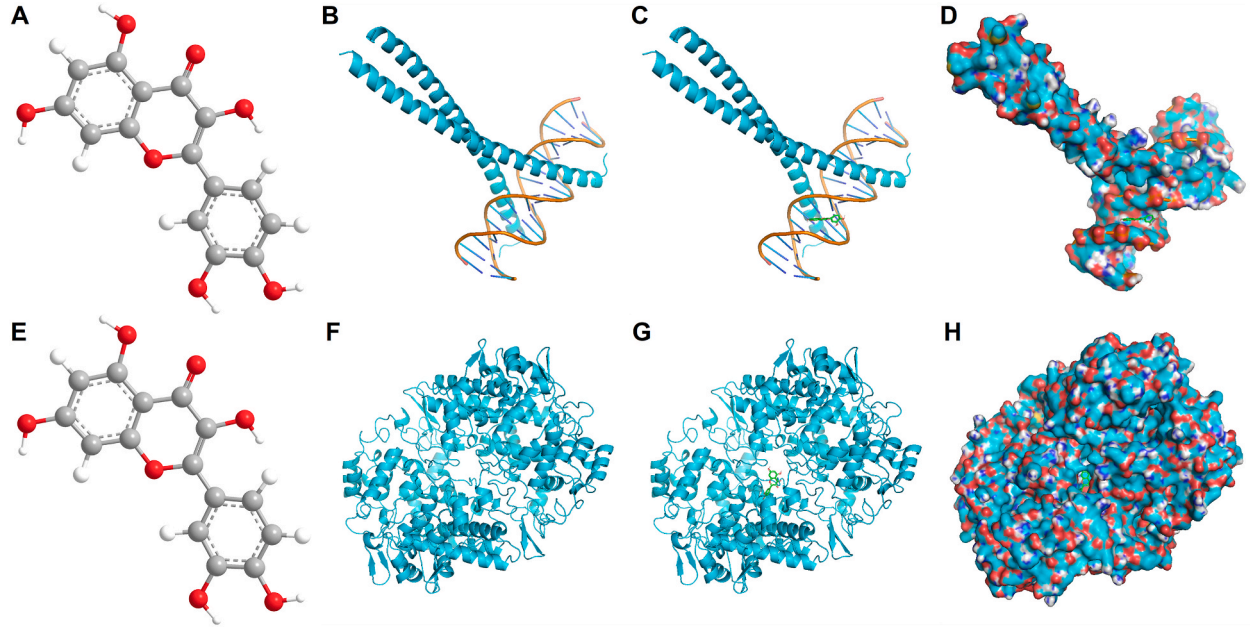

Fig. 7. Illustration of molecular docking simulations of JUN-Quercetin and PTGS2-Quercetin.
(**A**) 3D structure of quercetin. (**B**) 3D structure of JUN protein. (**C**) In the molecular docking simulations of JUN-quercetin, minimum affinity was −8.6 kcal/mol (**D**) molecular docking simulation of JUN-quercetin (displaying protein surface). (**E**) 3D structure of quercetin. (**F**) 3D structure of PTGS2 protein. (**G**) In the molecular docking simulations of PTGS2-quercetin, minimum affinity was −9.9 kcal/mol (**H**) molecular docking simulation of PTGS2-quercetin (displaying protein surface).

relative to the control group. Additionally, lung function metrics, including FEV1%, FEV1, FVC%, and FEV1/FVC ratio, were noticeably improved in the experimental group, without significant variation in adverse effects, compared with the control group. Given the strong correlation between clinical efficacy, lung function, and IPF prognosis, XFZYD showed promise in improving both symptoms and lung functions in IPF patients. This study, integrating TCM principles and evidence-based approaches, provides a solid basis for further investigation into the pharmacological actions of XFZYD in treating IPF.

We advanced our study by employing bioinformatics approaches to delve into the pharmacologic actions of XFZYD for IPF management. Microarray datasets were retrieved to pinpoint IPF-related target genes, and the network pharmacological methods were utilized to elucidate the pharmacological processes of XFZYD in IPF treatment. The GEO database, a rich source of openly accessible gene expression profiles, provides data and facilitates its integration for generating new hypotheses and insights [33]. The precision in identifying IPF-related target genes was enhanced through the examination of the GEO-retrieved microarray datasets. Network pharmacology, frequently employed in TCM research, allows for a detailed examination of herbal medicines and the identification of active pharmacodynamic ingredients. This methodology supports a shift in TCM from an expertise-based approach to an evidence-based healthcare paradigm [34]. Network pharmacology underscores the significance of multi-component treatments, aligning with the intrinsic characteristics (multi-component, multi-target, and multi-pathway) of TCM practices [35].

In our study, we recognized 254 target genes of XFZYD from the TCMSP and 1,566 DEGs from the GEO database. The intersection of these genes yielded 48 target genes of XFZYD for IPF treatment. Our GO functional analysis of BP enrichment highlighted the significant role of the genes in responses to nutrient, nutrients levels, extracellular stimulus and oxidative stress, regulation of body fluid levels, ECM organization, vasoconstriction, extracellular structure organization, negative regulation of blood vessel diameter, and cellular response to oxidative stress. Furthermore, GO CC functional enrichment demonstrated prominent enrichment of the XFZYD-associated target genes for IPF treatment in integral component of presynaptic membrane, plasma membrane raft, membrane microdomain, membrane region, caveola, intrinsic component of presynaptic membrane, ECM, intrinsic component of postsynaptic membrane, membrane raft, and integral component of postsynaptic membrane. The GO MF functional enrichment analysis showed the marked enrichment of the XFZYD-associated target genes for IPF treatment in protein heterodimerization activity, G protein-coupled amine receptor activity, CXCR chemokine receptor binding, heme binding, chemokine receptor binding, tetrapyrrole binding, protease binding, platelet-derived growth factor binding, oxidoreductase activity/acting on the CH-NH2 group of donors/oxygen as acceptor, and G protein-coupled receptor binding. These functions are closely associated with key pathological processes in IPF, such as aging, inflammation, cell proliferative, migratory, and apoptotic potential, thereby elucidating the pathogenic mechanisms of IPF [36–38].

The KEGG pathway enrichment analysis of XFZYD-associated target genes for IPF treatment revealed prominent enrichment several pathways, including the lipid and atherosclerosis, TNF signaling pathway, chemical carcinogenesis-receptor activation, IL-17 signaling pathway, Kaposi sarcoma-related herpesvirus infection, rheumatoid arthritis, fluid shear stress and atherosclerosis, AGE-RAGE signaling pathway in diabetes complications, chemical carcinogenesis-DNA adducts, and bladder cancer. These results

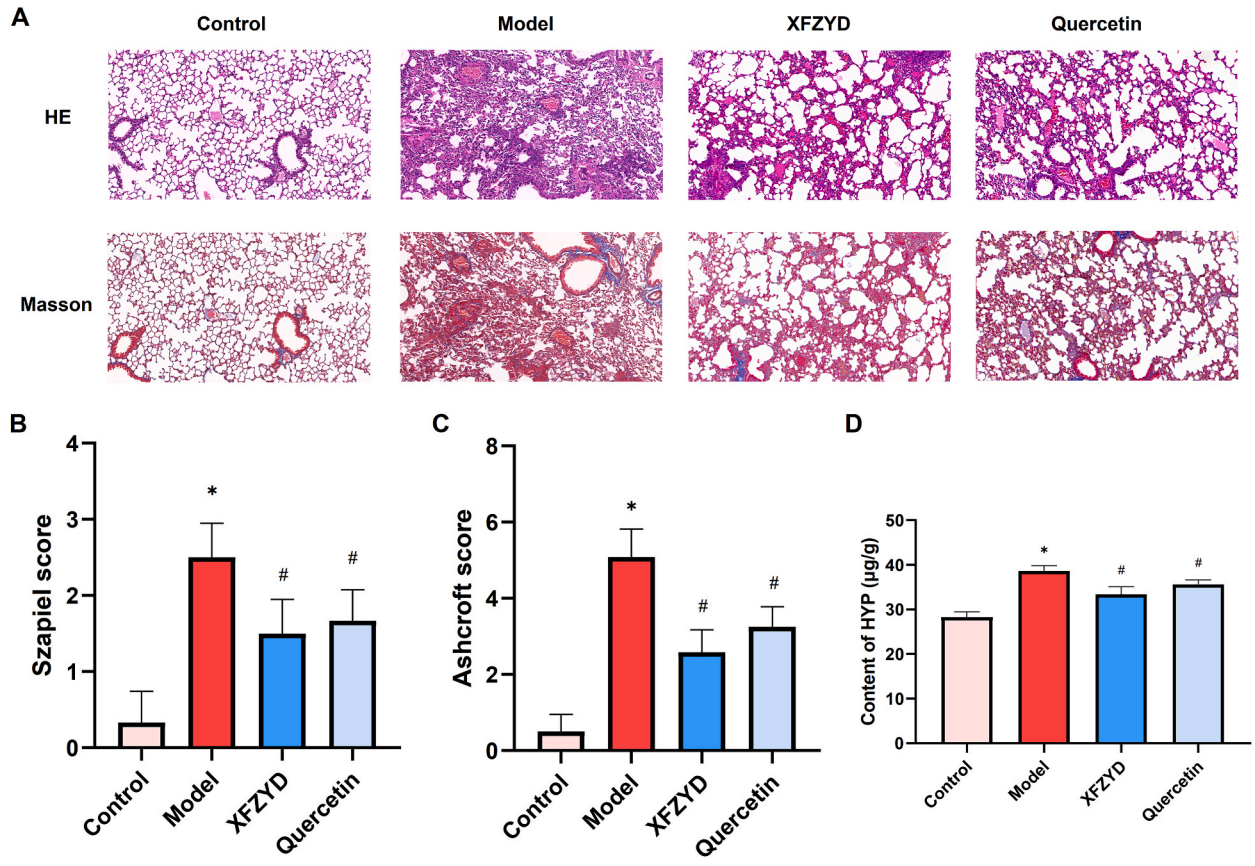

Fig. 8. Assessment of bleomycin-induced IPF model.
(**A**) Pathological alterations and the degree of PF were examined through HE and Masson staining across four groups: control, model, XFZYD-treated, and quercetin-treated groups (n = 6, scale bar × 200). (**B**) Szapiel score assessment. (**C**) Ashcroft score assessment. (**D**) Content of HYP. *P < 0.05 *vs.* Control group; #P < 0.05 *vs.* Model group.

pointed out the potential of XFZYD for IPF management through multiple pathways. Therefore, a more thorough investigation into these pathways and their associated target genes is warranted in the future study.

The present research proceeded to establish an ingredient-target network for XFZYD to pinpoint its active ingredients in the treatment of IPF. The network revealed interactions among 130 active ingredients across 48 intersecting target genes, implicating each herb in XFZYD as potentially beneficial in attenuating IPF progression. In addition, the active ingredients in SP and FC demonstrated significant prominence in the ingredient-target network. These results align with the TCM principles, where both SP and FC were recognized as 'monarch herbs,' known for their potent effects in XFZYD. This finding led us to pinpoint the key active ingredients in XFZYD for IPF management.

The key active ingredients in XFZYD for IPF treatment identified in our study included quercetin, kaempferol, stigmasterol, beta-carotene, luteolin, wogonin, beta-sitosterol, and medicarpin. The therapeutic action of XFZYD on IPF potentially results from the combined interaction of these active ingredients. Quercetin, for instance, is known to curtail bleomycin-induced lung fibrogenesis in mice [39] and mitigates PF by blocking the SphK1/S1P signaling pathway [40]. Its role in restoring the altered oxidation-reduction balance and diminishing inflammatory reactions could be beneficial for IPF patients [41]. The antioxidant activity of beta-carotene is correlated with oxidant and antioxidant balance, which is closely related to IPF [42,43]. Luteolin has demonstrated efficacy in experimental PF treatments *in vitro* and *in vivo* [44]. Beta-sitosterol can attenuate PF through suppression of epithelial-mesenchymal transition by inhibiting the TGF-β1/Snail pathway [45]. Nonetheless, the combined effect of these ingredients in IPF management remains under-explored and requires future in-depth research.

The PPI network for XFZYD in IPF treatment highlighted a variety of targeted actions. Key target genes/proteins included JUN, PTGS2, CCL2, HIF1A, MYC, CXCL8, SERPINE1, CCND1, VCAM1, and MMP3. PTGS2/COX2 is widely expressed in the metaplastic epithelium in pulmonary fibrous disorders [46], with COX2 expression observed to be lower in bronchiolar epithelial cells in the context of IPF than in controls [47]. COX2-PGE2 axis has dual roles in PF [48] and the augmented transcription of CCL2 in PF is linked to increased binding of transcription factors to AP-1 and nuclear factor κB (NF-κB) in the CCL2 promoter [49]. The CCL2-dependent macrophage activation may be significant for overall survival in patients with IPF [50]. A notable induction of CCL2 in the pulmonary epithelium is linked to proteinase-activated receptor-1-inducible CCL2 in individuals affected by PF [51]. The role of

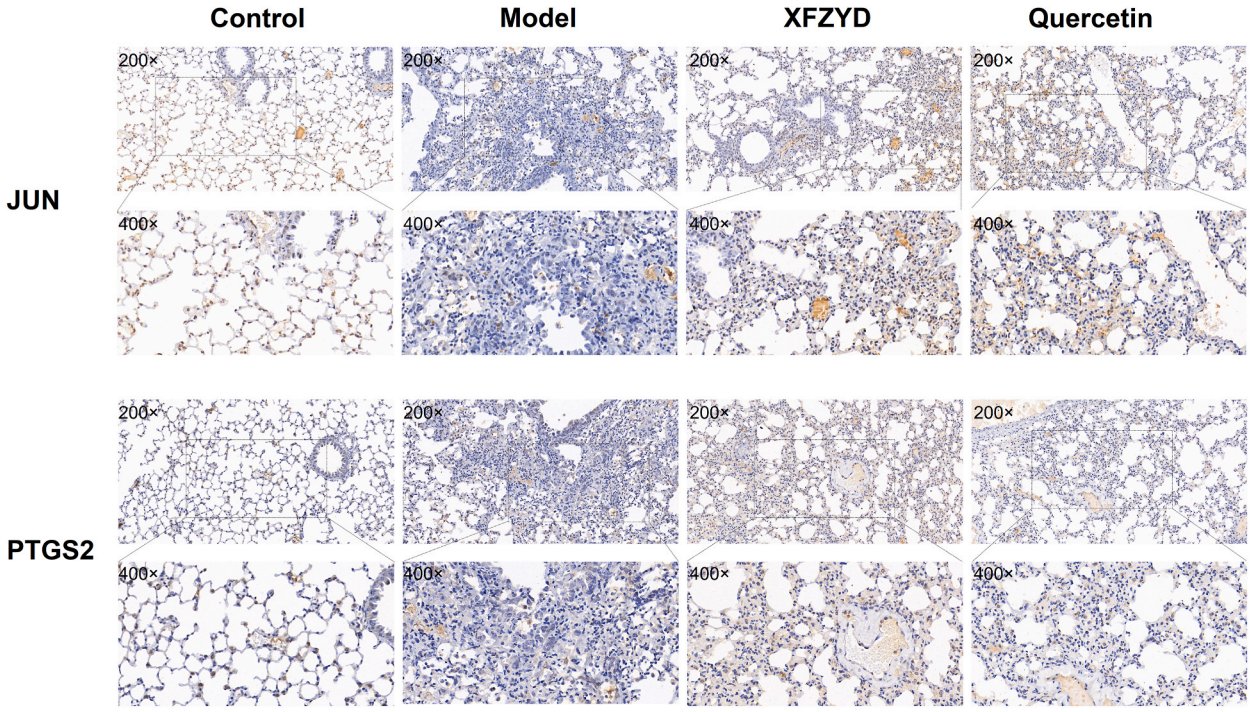

Fig. 9. Immunohistochemical evaluation of lung samples.
The levels of JUN and PTGS2 proteins in lung tissues were investigated using immunohistochemistry in the control, model, XFZYD-treated, and quercetin-treated groups (n = 6).

hypoxia-inducible factor 1α (HIF-1α) in regulating early PF, particularly due to paraquat exposure, involves the beta-catenin and Snail pathways [52]. Additionally, HIF-1α activation results in the elevation in ADORA2B receptor expression on conversely activated macrophages, contributing to PF progression [53]. The effectiveness of resveratrol in mitigating bleomycin-induced PF has been attributed to its inhibition of NF-κB and HIF-1α expression [54]. Acute exacerbations in the early phases of IPF are associated with heightened levels of IL-6 and IL-8 [55], with IL-8 actively participating in the fibrogenesis of mesenchymal progenitor cells in the context of IPF [56]. Both IL-1β and CXCL8 are crucial in driving chemotactic responses to bronchoalveolar lavage fluid [57]. Curcumin causes a decline in the expression of p53-PAI-1 in bleomycin-induced alveolar basal epithelial cells via IL-17A signaling inhibition-dependent mechanism [58]. The therapeutic action of nintedanib in bleomycin-induced PF involves suppressing neutrophil chemotaxis and endothelial cell activation. This effect is associated with increased GRK2 activity, decreased expression of VLA-4 and CXCR2 on neutrophils, and a decline in VCAM-1 expression in endothelial cells [59]. Matrix metalloproteinase 3 (MMP-3), a proteinase, has been implicated in the mediation of PF [60]. The correlation between these genes/proteins and IPF provides a foundation for ongoing research, including investigation into previously unexplored molecular pathways.

Furthermore, molecular docking corroborated the potential interactions between key active ingredients and corresponding target proteins in XFZYD for IPF management, thereby increasing the accuracy of the network analysis. Initial docking data unveiled strong binding affinities between the key active ingredients of XFZYD and their corresponding target proteins, indicating their potential as crucial foundational agents in the advancement of XFZYD for IPF treatment via associated signaling pathways. To validate this hypothesis, we conducted molecular docking studies focusing on quercetin with the top two target proteins, JUN and PTGS2. Experimental validation was subsequently conducted to assess the expression of JUN and PTGS2 in animal models in response to XFZYD and quercetin intervention. The results indicated that XFZYD and quercetin improved the alveolar structure, ameliorated PF, and influenced the expression of JUN and PTGS2 proteins in a bleomycin-induced IPF model. JUN and PTGS2 are closely related to the inflammatory pathway. We also measured the content of TNF-α, IL-6 and IL-1β in serum by enzyme-linked immuno sorbent assay (ELISA). The results showed that XFZYD and quercetin reduced the levels of TNF-α, IL-6 and IL-1β in serum (Supplementary Figure S6). These also provide the basis for further in-depth mechanistic research.

This study enhanced the evidence-based medicine to the effectiveness of XFZYD treatment for IPF and provided a basis for improving the prescription, which was consistent with TCM principles. Despite some of the research methodologies in the meta-analyses are of low quality, our extensive literature review underpins the reliability of our findings. Furthermore, we delineated the multifaceted mechanism of XFZYD for IPF management based on the influence of multiple active ingredients, target proteins, and signaling pathways. The application of bioinformatics techniques, including microarray analysis, network pharmacology, and molecular docking, facilitated our understanding of the pharmacological mechanisms of XFZYD for IPF management. Some chemicals and target genes could still be missing from these databases, although they are more thorough at present. These possible compounds, target

genes and pathways require additional investigation through experimental analysis. Molecular docking has preliminarily confirmed potential interactions between compounds and target proteins, providing insights for further mechanistic studies of the interactions. Experimental validation with animals substantiated the effectiveness of XFZYD and its key active ingredient, quercetin, in treating IPF through orchestrating the expression of key target proteins JUN and PTGS2. Our research, however, primarily focused on one compound and two target proteins for experiment validation, pointing to the need for broader research with the multi-compound and multi-target approach reflecting the characteristics of TCM. Although we have established initial interactions between the compounds and target proteins, further investigations are required to understand the precise underlying mechanisms of these interactions.

4. Conclusion

In conclusion, the present study provides robust evidence supporting the effectiveness of XFZYD for IPF treatment based on evidence-based medicine. Furthermore, this research clarifies the interactions among the associated pathways, target genes, and active ingredients of XFZYD for IPF management using bioinformatics tools. The findings highlight the multifaceted influence of multiple compounds, targets, and pathways. Moreover, molecular docking and animal experiments, particularly focusing on the impact of quercetin on JUN and PTGS2 proteins, underscore the significance of key compounds and target proteins in validating the therapeutic potential of XFZYD.

5. Materials and methods

5.1. Search for RCTs on the effectiveness of XFZYD for IPF treatment

The literature related to the efficacy of XFZYD on PF was systematically searched from China National Knowledge Infrastructure (https://www.cnki.net/), Wanfang Data (https://www.wanfangdata.com.cn/), Chinese Biomedical Literature database (http://www.sinomed.ac.cn/), Chongqing VIP Database (https://qikan.cqvip.com/), Cochrane Central Register of Controlled Trials (http://www.cochranelibrary.com/), and PubMed (https://pubmed.ncbi.nlm.nih.gov/) from the inception of each database to November 31, 2023. The search used a combination of the key term "pulmonary fibrosis" with either "Xuefu Zhuyu decoction" or "Xuefu Zhuyu Tang." This extensive search was not limited to titles and abstracts of articles, and full texts were also examined relevant information on these keywords. Manual examination of citations and references in the selected literature was also undertaken to pinpoint any additional qualified trials. This process continued until no further relevant research articles could be identified [61,62].

The studies selected for our analysis were required to satisfy the following criteria: study design as RCT, subjects diagnosed with IPF, intervention group receiving XFZYD, control group undergoing conventional therapy without TCM, and definitive outcome measures such as clinical effectiveness or lung function tests. Studies were excluded if they had incomplete outcome data or if the XFZYD prescription lacked essential components.

5.2. Data acquisition, quality evaluation, and meta-analysis

Data from the incorporated studies were extracted by two independent reviewers. The extracted key information encompassed the first author's name, publication year, sample size in each group, treatment modalities in the control and experimental groups, and research outcomes.

The assessment of bias risk was conducted based on the guidelines from the Cochrane Reviewers' Handbook for the seven metrics that could potentially introduce bias: generation of random sequences, allocation concealment, blinding of patient; blinding of assessor, incomplete outcome data, selective reporting, and other bias [63].

The extracted primary data were then systematically analyzed using RevMan 5.3 software, a tool of the Cochrane Collaboration, to perform meta-analyses on the effectiveness of XFZYD for IPF management.

5.3. Identification of active ingredients and target genes of XFZYD

To identify the active ingredients and target genes of XFZYD, the compounds were extracted from the 11 herbs (SP, FC, RPR, RC, RAB, RAS, RR, RP, FA, RB, and RG) using the TCMSP (https://tcmsp-e.com/tcmsp.php). This database offers a novel comprehensive pharmacological interface for Chinese herbal medicine for understanding the interactions among herbal medicines, targets, and diseases [64]. The active ingredients were pinpointed by applying thresholds for DL $\geq$ 0.18 and OB $\geq$ 30 %. OB indicates the absorption rate of active ingredients, and DL reflects the probability of a compound possessing similar physiological properties to conventional drugs [65,66].

The TCMSP was also utilized to identify target genes linked to the active ingredients. Subsequently, the target genes, using the query "*homo sapiens,*" were input into the UniProt (http://www.uniprot.org/), which is known for its extensive protein sequence data and annotation profiles [67]. Following this, official gene symbols were established as the identified target genes associated with XFZYD.

5.4. Exploration of microarray datasets and identification of DEGs for IPF research

Microarray datasets pertaining to IPF were retrieved in the GEO database (https://www.ncbi.nlm.nih.gov/gds/) at the National

Center for Biotechnology Information (NCBI). The search strategy was as follows: idiopathic pulmonary fibrosis [All Fields] AND "*Homo sapiens*"[porgn] AND ("gse"[Filter] AND "Expression profiling by array"[Filter]). The datasets comprising gene expression data from clinical IPF and normal samples were incorporated for further detailed examination.

The DEGs between IPF and normal samples in microarray datasets were identified through the application of the GEO2R online platform (https://www.ncbi.nlm.nih.gov/geo/geo2r/). The differential expression analysis was carried out using "GEOquery" and "limma" packages based on the processed data tables originally provided by submitters. DEGs were pinpointed through analysis of the data comparing IPF and normal samples with the cutoff criteria of $|\log2FC| > 1$ and adj P value < 0.05 [66,68].

5.5. Identification of target genes of XFZYD for IPF management

The target genes of XFZYD were matched to the DEGs in IPF studies. The target genes of XFZYD for IPF management were determined based on their intersection with these DEGs, which were visualized using the "VennDiagram" package of RGUI software.

5.6. Analyses of GO functional and KEGG pathway enrichment

The entrezIDs for the target genes were retrieved through the application of RGUI software and the "org.Hs.eg.db" package. We then proceeded with GO functional enrichment analysis, which includes BP, CC, and MF, using the "clusterProfiler" package. In addition, KEGG pathway enrichment analysis was conducted to explore the involved biological pathways [69].

5.7. Establishment of ingredient-target and PPI networks

An ingredient-target network was developed and analyzed utilizing the Cytoscape 3.6.0 software along with its NetworkAnalyzer tool [70]. In the network, the representation of nodes corresponded to ingredients and target genes, with edges symbolizing the interactions between these nodes. The degree of linkage in the network was used as a basis for further investigation into the ingredients and target genes. Key ingredients of XFZYD for IPF management were determined by analyzing the degree value associated with each ingredient in the network.

A PPI network was established following the incorporation of the target genes into the STRING database (https://string-db.org/). The application of the STRING database enables the identification of functional relationships in genome-wide experimental datasets [71]. For this analysis, "*homo sapiens*" was selected as the research species, the lowest interaction score was set at 0.4, and other settings were retained as default parameters to generate the PPI network. Subsequent topological analysis of the network was executed using Cytoscape and its NetworkAnalyzer function [70]. The primary target proteins of XFZYD for IPF management were pinpointed based on the degree value associated with each target protein.

5.8. Molecular docking validation

Molecular docking was implemented to corroborate the binding affinities between target proteins and corresponding compounds. The molecular structures of compounds and the structures of target proteins were retrieved from the PubChem database (https://pubchem.ncbi.nlm.nih.gov/) and the RCSB PDB database (http://www.rcsb.org/). The target proteins and compounds for molecular docking simulations were determined using AutoDock Vina and AutoDockTool 1.5.6 software [72].

5.9. In vivo experimental protocols

A total of 24 male C57BL/6 wild-type mice (aged 6–8 weeks, weighing 18–22 g) were obtained from the Animal Care Facility of Nanjing Medical University (Nanjing, China). The mice were housed under controlled environmental conditions and were provided with standard rodent chow and unrestricted access to water. In addition to untreated mice (Control group), the mice were administered with bleomycin alone (Model group) or in combination with XFZYD (XFZYD group) or quercetin (Quercetin group) ($n = 6$ for each group). For the induction of fibrosis, mice in the Model, XFZYD, and Quercetin groups were given 50 μl of bleomycin (5 mg/kg, HY-17565A, MedChemExpress China, Shanghai, China), and the Control group received an equivalent dose of normal saline through intratracheal injection using the endotracheal quantitative microsprayer aerosolizer (Shanghai Yuyan Instruments Co., Ltd., Shanghai, China) [73]. The control and model groups received intragastric administration of normal saline the day following the modeling procedure. In contrast, the treatment groups were subjected to daily administration of XFZYD or quercetin for a duration of 3 weeks. XFZYD granules utilized in the study were procured from Jiangyin Tianjiang Pharmaceutical Co., Ltd. (Jiangyin, China). The dosage of XFZYD was determined based on established clinical dosages and prior research findings [74]. In our study, the following dosages were administered: SP at 1.56 mg/g, FC, RAB, RAS and RR at 1.17 mg/g, RPR, FA and RG at 0.78 mg/g, RC and RP at 0.59 mg/g, and RB at 0.39 mg/g. These dosages were scaled based on an adult human equivalent for a 70 kg body weight using crude drug amounts of 12 g for SP, 9 g each for FC, RAB, RAS and RR, 6 g each for RPR, FA and RG, 4.5 g each for RC and RP, and 3 g for RB. Quercetin (HY-18085, MedChemExpress China, Shanghai, China) was administered at a dosage of 50 mg/kg, as established in prior research findings [40,75]. On day 21, mice were anesthetized and euthanized for subsequent experimental analyses. The experimental protocols were approved by the Ethics Committee for Animal Experiments of Nanjing University of Chinese Medicine (A211201).

5.10. Histopathological assay of lung tissues

On day 21, the mice were humanely euthanized, and lung specimens were extracted for histopathological analysis. Lung tissues were immersed in 10 % formaldehyde solution for 24 h to ensure proper fixation. Following this, the central sections of these tissues were embedded in paraffin. Thin slices of 5 μm were then obtained from these paraffin-embedded blocks using a microtome. The sections underwent HE and Masson staining to evaluate any lung tissue damage or morphological alterations. The Szapiel and Ashcroft scores were utilized to semi-quantitatively evaluate the histopathological changes in a blinded manner. The scoring systems facilitated the quantification of inflammatory cell infiltration, fibroblast growth, alveolar wall damage, and collagen deposition. The Szapiel score was determined on a scale of 0–3, whereas the Ashcroft score was based on a broader range of 0–8 [74,76,77]. Detailed criteria for both scoring systems are provided in Supplementary Table S7 (Szapiel score) and Supplementary Table S8 (Ashcroft score).

5.11. Content of HYP examination

HYP assay kit (A030-2-1) was purchased from Nanjing Jiancheng Bioengineering Institute (Nanjing, China). To measure the level of HYP, lung tissues were weighed and homogenated. Alkali hydrolysis assay was conducted to investigate the content of HYP. Hydrolytic liquid was added and the mixture was boiled in water in concordance with the instruction manual. The absorbance value was examined at 550 nm on a spectrophotometer (RT-6100, Rayto, Shenzhen, China).

5.12. Immunohistochemical assay of lung tissues

The investigation of relevant protein expression involved the application of immunohistochemistry. Following the deparaffinization process, paraffin sections underwent a 1-min treatment with 1.0 % periodate to block the activity of endogenous peroxidases. The paraffin sections were exposed to citrate buffer and microwaved for 10 min for antigen retrieval. The sections were allowed to cool down to ambient temperature and then rinsed with phosphate-buffered saline (PBS). Thereafter, a 30-min blocking step with normal goat serum at 37 °C was performed, followed by overnight incubation at 4 °C with primary antibodies (Aifang biological, Changsha, China) targeting the JUN antigen (AF00603) and PTGS2 antigen (AF03175). A negative control group was established using the remaining slide. The following day, the slides underwent three washes with PBS, and sections were subjected to a 10-min incubation with the secondary antibody at 37 °C. Following PBS washing, the sections underwent treatment with the streptavidin-biotin-peroxidase complex for 10 min. Diaminobenzidine was introduced as the visualizing agent, and nuclear staining was carried out using hematoxylin. A light microscope at a photo documentation facility (Olympus, Tokyo) was employed to examine the positive rate.

5.13. Measurement of inflammatory cytokines by ELISA

ELISA was performed to measure the content of TNF-α, IL-6 and IL-1β in serum. ELISA kit for TNF-α (AF2132-A), IL-6 (AF3066-A) and IL-1β (AF2040-A) were provided by Aifang biological (Changsha, China). The mice were sacrificed to collect the blood. Then, the samples were centrifuged (3500 rpm, 4 °C, 15 min) to gather supernatants. The inflammatory cytokines content was examined according to the manufacturer's protocol. The optical density was determined at 450 nm on a spectrophotometer (RT-6100, Rayto, Shenzhen, China).

5.14. Statistical analysis

Meta-analysis was executed utilizing the RevMan 5.3 software. The continuous data were presented as mean differences (MDs) with corresponding 95 % CIs, while dichotomous data were expressed as ORs with corresponding 95 % CIs. The degree of heterogeneity among the studies was evaluated using the Q test (P-value and I^2). A P value of <0.10 was indicative of significant heterogeneity. Studies with an $I^2 < 50$ % were considered to have low heterogeneity, whereas those with $I^2 \geq 50$ % were categorized as having high heterogeneity. The fixed effects model was applied for pooling data in cases without significant heterogeneity, while the random effect model was applied in the presence of heterogeneity. $P < 0.05$ was established as an indicator of statistical significance.

Statistical analyses pertinent to bioinformatics approaches were carried out using various bioinformatic tools accessed from dedicated websites, RGUI 3.6.1 software, and corresponding R packages. The cutoff criteria for DEG identification were set with $|\log2FC| > 1$ and adj $P < 0.05$. An adj $P < 0.05$ was designated as an indicator of statistical significance in the GO functional and KEGG pathway enrichment analyses.

All experimental data were analyzed with GraphPad Prism 8.0 software and were presented as mean ± standard deviation (SD). Shapiro–Wilk tests were performed to determine the normality of the data distribution. One-way ANOVA with Tukey's multiple comparisons test was used to analyze the differences among groups for normally distributed data, and Kruskal-Wallis test with Dunn's multiple comparisons test was used for data not conforming to a normal distribution. $P < 0.05$ was established as an indicator of statistical significance.

Ethics statement

All animal care and experimental procedures complied with the guidelines approved by the Ethics Committee for Animal Experiments of Nanjing University of Chinese Medicine (A211201).

GEO belongs to public databases. The patients involved in the database have obtained ethical approve. Users can download data for free for research and publish relevant articles.

Data availability

Publicly available datasets were analyzed in this study. Gene Expression Omnibus (GEO; http://www.ncbi.nlm.nih.gov/geo/) (Accessions: GSE2052, GSE21369, GSE24206, and GSE53845). The data generated and/or analyzed during the current study are available from the corresponding author upon a reasonable request. Main data from this study are also included in this published article (and its Supplementary Information files).

Funding

This work was supported by the Health "Three Famous" Strategy Talent Project of Wuxi City: the “Double Hundred” Young and Middle-aged Medical and Health Top-notch Talents Training Plan of Wuxi City (HB2023106 to Yufeng Zhang), the Young and Middle-aged Health Excellent Talents Training Plan of Jiangyin City (JYROYT202311 to Qingqing Xia, JYOYT202311 to Yufeng Zhang), the “ChengXing” Talents Training Plan of Jiangyin Hospital of Traditional Chinese Medicine (2022 to Qingqing Xia, 2022 to Yufeng Zhang), the Scientific Research Project of Jiangyin Association of Chinese Medicine (Y202205 to Yufeng Zhang), the Science and Technology Innovation Special Fund Project of Jiangyin City (JY0603A011014230012PB to Chenjing Zhu), the Scientific Research Project of Wuxi Municipal Health Commission (T202130 to Weilong Jiang, M202154 to Yufeng Zhang), Medical Science and Technology Development Plan Project of Yancheng City (YK2020046 to Huizhe Zhang), Natural Science Foundation of Nanjing University of Chinese Medicine (XZR2021096 to Huizhe Zhang, XZR2023081 to Xiaodong Hu, XZR2021099 to Yufeng Zhang) and the Traditional Chinese Medicine Science and Technology Development Plan Project of Jiangsu Province (MS2022108 to Huizhe Zhang, ZT202113 to Haibing Hua, MS2022060 to Yufeng Zhang).

CRediT authorship contribution statement

Huizhe Zhang: Writing – original draft, Visualization, Validation, Supervision, Software, Project administration, Methodology, Funding acquisition, Data curation, Conceptualization, Writing – review & editing. **Haibing Hua:** Writing – review & editing, Writing – original draft, Resources, Project administration, Methodology, Investigation, Funding acquisition, Formal analysis, Data curation, Conceptualization. **Jian Liu:** Software, Resources, Project administration, Methodology, Investigation, Funding acquisition, Formal analysis, Data curation, Writing – original draft, Writing – review & editing. **Cong Wang:** Methodology, Investigation, Formal analysis, Data curation. **Chenjing Zhu:** Software, Resources, Methodology, Formal analysis, Data curation. **Qingqing Xia:** Validation, Software, Resources, Methodology, Investigation, Funding acquisition, Formal analysis, Data curation. **Weilong Jiang:** Software, Resources, Methodology, Investigation, Funding acquisition, Formal analysis, Data curation. **Xiangjin Cheng:** Writing – review & editing, Writing – original draft, Validation, Supervision, Software, Resources, Project administration, Methodology, Investigation, Formal analysis, Data curation, Conceptualization. **Xiaodong Hu:** Writing – review & editing, Writing – original draft, Visualization, Validation, Supervision, Software, Resources, Project administration, Methodology, Investigation, Funding acquisition, Formal analysis, Data curation, Conceptualization. **Yufeng Zhang:** Writing – review & editing, Writing – original draft, Visualization, Validation, Supervision, Software, Resources, Project administration, Methodology, Investigation, Funding acquisition, Formal analysis, Data curation, Conceptualization.

Declaration of competing interest

The authors declare that they have no known competing financial interests or personal relationships that could have appeared to influence the work reported in this paper.

Acknowledgments

We extend our sincere thanks to the providers of the online database platform and the analytical software used in this study.

Appendix A. Supplementary data

Supplementary data to this article can be found online at https://doi.org/10.1016/j.heliyon.2024.e38122.

References

[1] G. Raghu, M. Remy-Jardin, J.L. Myers, L. Richeldi, C.J. Ryerson, D.J. Lederer, J. Behr, V. Cottin, S.K. Danoff, F. Morell, K.R. Flaherty, A. Wells, F.J. Martinez, A. Azuma, T.J. Bice, D. Bouros, K.K. Brown, H.R. Collard, A. Duggal, L. Galvin, Y. Inoue, R.G. Jenkins, T. Johkoh, E.A. Kazerooni, M. Kitaichi, S.L. Knight,

G. Mansour, A.G. Nicholson, S. Pipavath, I. Buendia-Roldan, M. Selman, W.D. Travis, S. Walsh, K.C. Wilson, Diagnosis of idiopathic pulmonary fibrosis. An official ATS/ERS/JRS/ALAT clinical practice guideline, Am. J. Respir. Crit. Care Med. 198 (2018) e44–e68, https://doi.org/10.1164/rccm.201807-1255ST.
[2] G. Raghu, M. Remy-Jardin, L. Richeldi, C.C. Thomson, Y. Inoue, T. Johkoh, M. Kreuter, D.A. Lynch, T.M. Maher, F.J. Martinez, M. Molina-Molina, J.L. Myers, A. G. Nicholson, C.J. Ryerson, M.E. Strek, L.K. Troy, M. Wijsenbeek, M.J. Mammen, T. Hossain, B.D. Bissell, D.D. Herman, S.M. Hon, F. Kheir, Y.H. Khor, M. Macrea, K.M. Antoniou, D. Bouros, I. Buendia-Roldan, F. Caro, B. Crestani, L. Ho, J. Morisset, A.L. Olson, A. Podolanczuk, V. Poletti, M. Selman, T. Ewing, S. Jones, S.L. Knight, M. Ghazipura, K.C. Wilson, Idiopathic pulmonary fibrosis (an update) and progressive pulmonary fibrosis in adults: an official ATS/ERS/JRS/ALAT clinical practice guideline, Am. J. Respir. Crit. Care Med. 205 (2022) e18–e47, https://doi.org/10.1164/rccm.202202-0399ST.
[3] H. Kim, S.H. Yoon, H. Hong, S. Hahn, J.M. Goo, Diagnosis of idiopathic pulmonary fibrosis in a possible usual interstitial pneumonia pattern: a meta-analysis, Sci. Rep. 8 (2018) 15886, https://doi.org/10.1038/s41598-018-34230-z.
[4] Y. Zhang, L. Gu, Q. Xia, L. Tian, J. Qi, M. Cao, Radix astragali and radix angelicae sinensis in the treatment of idiopathic pulmonary fibrosis: a systematic review and meta-analysis, Front. Pharmacol. 11 (2020) 415, https://doi.org/10.3389/fphar.2020.00415.
[5] H. Zhang, C. Wang, Y. Zhang, Progress of radix astragali and radix angelicae sinensis in the treatment of idiopathic pulmonary fibrosis, TMR Integr Med 6 (2022) e22001–e22036, https://doi.org/10.53388/TMRIM202206024.
[6] Y. Zhang, W. Jiang, Q. Xia, J. Qi, M. Cao, Pharmacological mechanism of Astragalus and Angelica in the treatment of idiopathic pulmonary fibrosis based on network pharmacology, Eur J Integr Med 32 (2019) 101003, https://doi.org/10.1016/j.eujim.2019.101003.
[7] M. Zhou, C. Ye, Q. Liang, Q. Pei, F. Xu, H. Wen, Yiqi yangyin huoxue method in treating idiopathic pulmonary fibrosis: a systematic review and Meta-Analysis of randomized controlled trials, Evid Based Complement Alternat Med 2020 (2020) 8391854, https://doi.org/10.1155/2020/8391854.
[8] Q. Wu, Y. Zhou, F.C. Feng, X.M. Zhou, Effectiveness and safety of Chinese medicine for idiopathic pulmonary fibrosis: a systematic review and Meta-Analysis, Chin. J. Integr. Med. 25 (2019) 778–784, https://doi.org/10.1007/s11655-017-2429-5.
[9] S. Yang, W. Cui, M. Wang, L. Xing, Y. Wang, P. Zhu, Q. Qu, Q. Tang, Bufei decoction alleviated Bleomycin-Induced idiopathic pulmonary fibrosis in mice by Anti-Inflammation, Evid Based Complement Alternat Med 2020 (2020) 7483278, https://doi.org/10.1155/2020/7483278.
[10] F. Chen, P.L. Wang, X.S. Fan, J.H. Yu, Y. Zhu, Z.H. Zhu, Effect of Renshen Pingfei Decoction, a traditional Chinese prescription, on IPF induced by Bleomycin in rats and regulation of TGF-beta1/Smad3, J. Ethnopharmacol. 186 (2016) 289–297, https://doi.org/10.1016/j.jep.2016.03.051.
[11] T. Yi, P. Gao, M. Hou, H. Lv, M. Huang, S. Gao, J. He, D. Yang, W. Chen, T. Zhu, C. Yu, F. Liu, H. Yin, S. Jin, The mechanisms underlying the actions of Xuefu Zhuyu decoction pretreatment against neurological deficits after ischemic stroke in mice: the mediation of glymphatic function by aquaporin-4 and its anchoring proteins, Front. Pharmacol. 13 (2022) 1053253, https://doi.org/10.3389/fphar.2022.1053253.
[12] J. Yuan, F. Yan, W. Li, G. Yuan, Network pharmacological analysis of Xuefu Zhuyu decoction in the treatment of atherosclerosis, Front. Pharmacol. 13 (2022) 1069704, https://doi.org/10.3389/fphar.2022.1069704.
[13] Y.Q. Guo, J. Yang, Clinical study of Xuefu Zhuyu decoction combined with compression and atomization inhalation of Pulmicort respules for idiopathic pulmonary interstitial fibrosis, J. Emerg. Tradit. Chin. Med. 18 (2009) 1590–1591, https://doi.org/10.3969/j.issn.1004-745X.2009.10.013.
[14] Y.Y. Song, Clinical effect of Xuefu Zhuyu decoction treatment in elderly patients with idiopathic pulmonary fibrosis, J Clin Med Pract 20 (2016) 155, https://doi.org/10.7619/jcmp.201609052.
[15] Q. Wang, Y.J. Guan, Y. Qi, M.F. Li, M. Li, Experimental study on the mechanism of xuefu zhuyu decoction on the expression of smad-3 and MMP-7 in rats with pulmonary fibrosis, J Liaoning Univ Trad Chin Med 21 (2019) 36–39, https://doi.org/10.13194/j.issn.1673-842x.2019.09.010.
[16] Y.B. Wu, H. Xie, J.Y. Wang, K.P. Xiao, X.Y. Pan, H.J. Yang, H.L. Zhao, J.L. Qu, Effects of xuefu zhuyu tang on epithelial-mesenchymal transition of lung tissue in pulmonary fibrosis model rats and mechanism study, Chin. J. Ethnomed. Ethnopharmacy 29 (2020) 11–16, https://doi.org/10.3969/j.issn.1007-8517.2020.17.zgmzmjyyzz202017005.
[17] R.J. Ju, Y.T. Xu, M. Guo, Z.W. L, Meta analysis of the effectiveness and safety of xuefu zhuyu decoction in the treatment of pulmonary fibrosis, Clin J Trad Chin Med 33 (2021) 1125–1129, https://doi.org/10.16448/j.cjtcm.2021.0628.
[18] L.L. Wang, Clinical therapeutic effect of prednisone combined with Xuefu Zhuyu Decoction in the treatment of idiopathic pulmonary fibrosis, J Pract Trad Chin Med 33 (2017) 1147–1148, https://doi.org/10.3969/j.issn.1004-2814.2017.10.024.
[19] M. Wang, Study on clinical efficacy of Xuefu Zhuyu decoction combined with western medicine in the treatment of pulmonary interstitial fibrosis, Shaanxi J Trad Chin Med 40 (2019) 893–895, https://doi.org/10.3969/j.issn.1000-7369.2019.07.022.
[20] W.J. Tang, K.L. Chen, W. Xiao, P.C. Zhou, W.J. Wang, Experience of treating idiopathic pulmonary interstitial fibrosis by lung tonifying and blood activating method, Practical Clin. J. Integrated Tradit. Chin. West. Med. 19 (2019) 118–119, https://doi.org/10.13638/j.issn.1671-4040.2019.04.060.
[21] J. Yuan, W. Yan, X. Wang, M. Gao, L. J, J. Zhao, Efficacy and safety of Xuefu Zhuyu Decoction combined with N-acetylcysteine in the treatment of idiopathic pulmonary fibrosis, J Tianjin Univ Trad Chin Med 39 (2020) 55–58, https://doi.org/10.11656/j.issn.1673-9043.2020.01.13.
[22] X.M. Wang, Y. Zhang, H.P. Kim, Z. Zhou, C.A. Feghali-Bostwick, F. Liu, E. Ifedigbo, X. Xu, T.D. Oury, N. Kaminski, A.M. Choi, Caveolin-1: a critical regulator of lung fibrosis in idiopathic pulmonary fibrosis, J. Exp. Med. 203 (2006) 2895–2906, https://doi.org/10.1084/jem.20061536.
[23] A. Pardo, K. Gibson, J. Cisneros, T.J. Richards, Y. Yang, C. Becerril, S. Yousem, I. Herrera, V. Ruiz, M. Selman, N. Kaminski, Up-regulation and profibrotic role of osteopontin in human idiopathic pulmonary fibrosis, PLoS Med. 2 (2005) e251, https://doi.org/10.1371/journal.pmed.0020251.
[24] J.M. Englert, L.E. Hanford, N. Kaminski, J.M. Tobolewski, R.J. Tan, C.L. Fattman, L. Ramsgaard, T.J. Richards, I. Loutaev, P.P. Nawroth, M. Kasper, A. Bierhaus, T.D. Oury, A role for the receptor for advanced glycation end products in idiopathic pulmonary fibrosis, Am. J. Pathol. 172 (2008) 583–591, https://doi.org/10.2353/ajpath.2008.070569.
[25] J.H. Cho, R. Gelinas, K. Wang, A. Etheridge, M.G. Piper, K. Batte, D. Dakhallah, J. Price, D. Bornman, S. Zhang, C. Marsh, D. Galas, Systems biology of interstitial lung diseases: integration of mRNA and microRNA expression changes, BMC Med. Genom. 4 (2011) 8, https://doi.org/10.1186/1755-8794-4-8.
[26] E.B. Meltzer, W.T. Barry, T.A. D'Amico, R.D. Davis, S.S. Lin, M.W. Onaitis, L.D. Morrison, T.A. Sporn, M.P. Steele, P.W. Noble, Bayesian probit regression model for the diagnosis of pulmonary fibrosis: proof-of-principle, BMC Med. Genom. 4 (2011) 70, https://doi.org/10.1186/1755-8794-4-70.
[27] D.J. DePianto, S. Chandriani, A.R. Abbas, G. Jia, E.N. N'Diaye, P. Caplazi, S.E. Kauder, S. Biswas, S.K. Karnik, C. Ha, Z. Modrusan, M.A. Matthay, J. Kukreja, H. R. Collard, J.G. Egen, P.J. Wolters, J.R. Arron, Heterogeneous gene expression signatures correspond to distinct lung pathologies and biomarkers of disease severity in idiopathic pulmonary fibrosis, Thorax 70 (2015) 48–56, https://doi.org/10.1136/thoraxjnl-2013-204596.
[28] J.J. Swigris, D.A. Andrae, T. Churney, N. Johnson, M.B. Scholand, E.S. White, A. Matsui, K. Raimundo, C.J. Evans, Development and initial validation analyses of the living with idiopathic pulmonary fibrosis questionnaire, Am. J. Respir. Crit. Care Med. 202 (2020) 1689–1697, https://doi.org/10.1164/rccm.202002-0415OC.
[29] N. Lechtzin, M.E. Hilliard, M.R. Horton, Validation of the Cough Quality-of-Life Questionnaire in patients with idiopathic pulmonary fibrosis, Chest 143 (2013) 1745–1749, https://doi.org/10.1378/chest.12-2870.
[30] Y. Zhang, P. Lu, H. Qin, Y. Zhang, X. Sun, X. Song, J. Liu, H. Peng, Y. Liu, E.O. Nwafor, J. Li, Z. Liu, Traditional Chinese medicine combined with pulmonary drug delivery system and idiopathic pulmonary fibrosis: rationale and therapeutic potential, Biomed. Pharmacother. 133 (2021) 111072, https://doi.org/10.1016/j.biopha.2020.111072.
[31] S. Zhang, Z.L. Chen, Y.P. Tang, J.L. Duan, K.W. Yao, Efficacy and safety of Xue-Fu-Zhu-Yu decoction for patients with coronary heart disease: a systematic review and Meta-Analysis, Evid Based Complement Alternat Med 2021 (2021) 9931826, https://doi.org/10.1155/2021/9931826.
[32] S. Wang, X.J. Qiu, The efficacy of Xue Fu Zhu Yu prescription for hyperlipidemia: a meta-analysis of randomized controlled trials, Compl. Ther. Med. 43 (2019) 218–226, https://doi.org/10.1016/j.ctim.2019.02.008.
[33] D. Toro-Dominguez, J. Martorell-Marugan, R. Lopez-Dominguez, A. Garcia-Moreno, V. Gonzalez-Rumayor, M.E. Alarcon-Riquelme, P. Carmona-Saez, ImaGEO: integrative gene expression meta-analysis from GEO database, Bioinformatics 35 (2019) 880–882, https://doi.org/10.1093/bioinformatics/bty721.
[34] S. Li, B. Zhang, Traditional Chinese medicine network pharmacology: theory, methodology and application, Chin. J. Nat. Med. 11 (2013) 110–120, https://doi.org/10.1016/S1875-5364(13)60037-0.
[35] L. Zhao, H. Zhang, N. Li, J. Chen, H. Xu, Y. Wang, Q. Liang, Network pharmacology, a promising approach to reveal the pharmacology mechanism of Chinese medicine formula, J. Ethnopharmacol. 309 (2023) 116306, https://doi.org/10.1016/j.jep.2023.116306.

[36] S.L. Brody, S.P. Gunsten, H.P. Luehmann, D.H. Sultan, M. Hoelscher, G.S. Heo, J. Pan, J.R. Koenitzer, E.C. Lee, T. Huang, C. Mpoy, S. Guo, R. Laforest, A. Salter, T.D. Russell, A. Shifren, C. Combadiere, K.J. Lavine, D. Kreisel, B.D. Humphreys, B.E. Rogers, D.S. Gierada, D.E. Byers, R.J. Gropler, D.L. Chen, J.J. Atkinson, Y. Liu, Chemokine receptor 2-targeted molecular imaging in pulmonary fibrosis. A clinical trial, Am. J. Respir. Crit. Care Med. 203 (2021) 78–89, https://doi.org/10.1164/rccm.202004-1132OC.
[37] S. Kolahian, I.E. Fernandez, O. Eickelberg, D. Hartl, Immune mechanisms in pulmonary fibrosis, Am. J. Respir. Cell Mol. Biol. 55 (2016) 309–322, https://doi.org/10.1165/rcmb.2016-0121TR.
[38] B.J. Moss, S.W. Ryter, I.O. Rosas, Pathogenic mechanisms underlying idiopathic pulmonary fibrosis, Annu. Rev. Pathol. 17 (2022) 515–546, https://doi.org/10.1146/annurev-pathol-042320-030240.
[39] A.W. Boots, C. Veith, C. Albrecht, R. Bartholome, M.J. Drittij, S. Claessen, A. Bast, M. Rosenbruch, L. Jonkers, F.J. van Schooten, R. Schins, The dietary antioxidant quercetin reduces hallmarks of bleomycin-induced lung fibrogenesis in mice, BMC Pulm. Med. 20 (2020) 112, https://doi.org/10.1186/s12890-020-1142-x.
[40] X. Zhang, Y. Cai, W. Zhang, X. Chen, Quercetin ameliorates pulmonary fibrosis by inhibiting SphK1/S1P signaling, Biochem. Cell. Biol. 96 (2018) 742–751, https://doi.org/10.1139/bcb-2017-0302.
[41] C. Veith, M. Drent, A. Bast, F.J. van Schooten, A.W. Boots, The disturbed redox-balance in pulmonary fibrosis is modulated by the plant flavonoid quercetin, Toxicol. Appl. Pharmacol. 336 (2017) 40–48, https://doi.org/10.1016/j.taap.2017.10.001.
[42] Y. Miyake, S. Sasaki, T. Yokoyama, K. Chida, A. Azuma, T. Suda, S. Kudoh, N. Sakamoto, K. Okamoto, G. Kobashi, M. Washio, Y. Inaba, H. Tanaka, Vegetable, fruit, and cereal intake and risk of idiopathic pulmonary fibrosis in Japan, Ann. Nutr. Metab. 48 (2004) 390–397, https://doi.org/10.1159/000082465.
[43] I. Rahman, S.K. Biswas, A. Kode, Oxidant and antioxidant balance in the airways and airway diseases, Eur. J. Pharmacol. 533 (2006) 222–239, https://doi.org/10.1016/j.ejphar.2005.12.087.
[44] C.Y. Chen, W.H. Peng, L.C. Wu, C.C. Wu, S.L. Hsu, Luteolin ameliorates experimental lung fibrosis both in vivo and in vitro: implications for therapy of lung fibrosis, J. Agric. Food Chem. 58 (2010) 11653–11661, https://doi.org/10.1021/jf1031668.
[45] Y.J. Park, I.J. Bang, M.H. Jeong, H.R. Kim, D.E. Lee, J.H. Kwak, K.H. Chung, Effects of beta-sitosterol from corn silk on TGF-beta1-induced epithelial-mesenchymal transition in lung alveolar epithelial cells, J. Agric. Food Chem. 67 (2019) 9789–9795, https://doi.org/10.1021/acs.jafc.9b02730.
[46] E. Lappi-Blanco, R. Kaarteenaho-Wiik, P.K. Maasilta, S. Anttila, P. Paakko, H.J. Wolff, COX-2 is widely expressed in metaplastic epithelium in pulmonary fibrous disorders, Am. J. Clin. Pathol. 126 (2006) 717–724, https://doi.org/10.1309/PFGX-CLNG-2N17-PJX9.
[47] D.K. Petkova, C.A. Clelland, J.E. Ronan, S. Lewis, A.J. Knox, Reduced expression of cyclooxygenase (COX) in idiopathic pulmonary fibrosis and sarcoidosis, Histopathology 43 (2003) 381–386, https://doi.org/10.1046/j.1365-2559.2003.01718.x.
[48] T. Bormann, R. Maus, J. Stolper, D. Jonigk, T. Welte, J. Gauldie, M. Kolb, U.A. Maus, Role of the COX2-PGE(2) axis in S. Pneumoniae-induced exacerbation of experimental fibrosis, Am. J. Physiol. Lung Cell Mol. Physiol. 320 (2021) L377–L392, https://doi.org/10.1152/ajplung.00024.2020.
[49] X. Deng, M. Xu, C. Yuan, L. Yin, X. Chen, X. Zhou, G. Li, Y. Fu, C.A. Feghali-Bostwick, L. Pang, Transcriptional regulation of increased CCL2 expression in pulmonary fibrosis involves nuclear factor-kappaB and activator protein-1, Int. J. Biochem. Cell Biol. 45 (2013) 1366–1376, https://doi.org/10.1016/j.biocel.2013.04.003.
[50] X. Gui, X. Qiu, Y. Tian, M. Xie, H. Li, Y. Gao, Y. Zhuang, M. Cao, H. Ding, J. Ding, Y. Zhang, H. Cai, Prognostic value of IFN-gamma, sCD163, CCL2 and CXCL10 involved in acute exacerbation of idiopathic pulmonary fibrosis, Int. Immunopharm. 70 (2019) 208–215, https://doi.org/10.1016/j.intimp.2019.02.039.
[51] P.F. Mercer, R.H. Johns, C.J. Scotton, M.A. Krupiczojc, M. Konigshoff, D.C. Howell, R.J. McAnulty, A. Das, A.J. Thorley, T.D. Tetley, O. Eickelberg, R. C. Chambers, Pulmonary epithelium is a prominent source of proteinase-activated receptor-1-inducible CCL2 in pulmonary fibrosis, Am. J. Respir. Crit. Care Med. 179 (2009) 414–425, https://doi.org/10.1164/rccm.200712-1827OC.
[52] Y. Zhu, J. Tan, H. Xie, J. Wang, X. Meng, R. Wang, HIF-1alpha regulates EMT via the Snail and beta-catenin pathways in paraquat poisoning-induced early pulmonary fibrosis, J. Cell Mol. Med. 20 (2016) 688–697, https://doi.org/10.1111/jcmm.12769.
[53] K. Philip, T.W. Mills, J. Davies, N.Y. Chen, H. Karmouty-Quintana, F. Luo, J.G. Molina, J. Amione-Guerra, N. Sinha, A. Guha, H.K. Eltzschig, M.R. Blackburn, HIF1A up-regulates the ADORA2B receptor on alternatively activated macrophages and contributes to pulmonary fibrosis, FASEB J 31 (2017) 4745–4758, https://doi.org/10.1096/fj.201700219R.
[54] Z. Wang, X. Li, H. Chen, L. Han, X. Ji, Q. Wang, L. Wei, Y. Miu, J. Wang, J. Mao, Z. Zhang, Resveratrol alleviates bleomycin-induced pulmonary fibrosis via suppressing HIF-1alpha and NF-kappaB expression, Aging (Albany NY) 13 (2021) 4605–4616, https://doi.org/10.18632/aging.202420.
[55] S.A. Papiris, I.P. Tomos, A. Karakatsani, A. Spathis, I. Korbila, A. Analitis, L. Kolilekas, K. Kagouridis, S. Loukides, P. Karakitsos, E.D. Manali, High levels of IL-6 and IL-8 characterize early-on idiopathic pulmonary fibrosis acute exacerbations, Cytokine 102 (2018) 168–172, https://doi.org/10.1016/j.cyto.2017.08.019.
[56] L. Yang, J. Herrera, A. Gilbertsen, H. Xia, K. Smith, A. Benyumov, P.B. Bitterman, C.A. Henke, IL-8 mediates idiopathic pulmonary fibrosis mesenchymal progenitor cell fibrogenicity, Am. J. Physiol. Lung Cell Mol. Physiol. 314 (2018) L127–L136, https://doi.org/10.1152/ajplung.00200.2017.
[57] A.G. Richter, G.D. Perkins, A. Chavda, E. Sapey, L. Harper, D.R. Thickett, Neutrophil chemotaxis in granulomatosis with polyangiitis (Wegener's) and idiopathic pulmonary fibrosis, Eur. Respir. J. 38 (2011) 1081–1088, https://doi.org/10.1183/09031936.00161910.
[58] M.M. Gouda, A. Prabhu, Y.P. Bhandary, Curcumin alleviates IL-17A-mediated p53-PAI-1 expression in bleomycin-induced alveolar basal epithelial cells, J. Cell. Biochem. 119 (2018) 2222–2230, https://doi.org/10.1002/jcb.26384.
[59] W.C. Chen, N.J. Chen, H.P. Chen, W.K. Yu, V.Y. Su, H. Chen, H.H. Wu, K.Y. Yang, Nintedanib reduces neutrophil chemotaxis via activating GRK2 in Bleomycin-Induced pulmonary fibrosis, Int. J. Mol. Sci. 21 (2020), https://doi.org/10.3390/ijms21134735.
[60] C.M. Yamashita, L. Dolgonos, R.L. Zemans, S.K. Young, J. Robertson, N. Briones, T. Suzuki, M.N. Campbell, J. Gauldie, D.C. Radisky, D.W. Riches, G. Yu, N. Kaminski, C.A. McCulloch, G.P. Downey, Matrix metalloproteinase 3 is a mediator of pulmonary fibrosis, Am. J. Pathol. 179 (2011) 1733–1745, https://doi.org/10.1016/j.ajpath.2011.06.041.
[61] Q. Xia, M. Liu, H. Li, L. Tian, J. Qi, Y. Zhang, Network pharmacology strategy to investigate the pharmacological mechanism of HuangQiXiXin decoction on cough variant asthma and Evidence-Based medicine approach validation, Evid Based Complement Alternat Med 2020 (2020) 3829092, https://doi.org/10.1155/2020/3829092.
[62] C. Wang, Q. Xia, B. Hu, W. Jiang, H. Zhang, The effectiveness and safety of huangqi xixin decoction for cough variant asthma: a systematic review and Meta-Analysis, Evid Based Complement Alternat Med 2022 (2022) 9492100, https://doi.org/10.1155/2022/9492100.
[63] J.P. Higgins, D.G. Altman, P.C. Gotzsche, P. Juni, D. Moher, A.D. Oxman, J. Savovic, K.F. Schulz, L. Weeks, J.A. Sterne, The Cochrane Collaboration's tool for assessing risk of bias in randomised trials, BMJ 343 (2011) d5928, https://doi.org/10.1136/bmj.d5928.
[64] J. Ru, P. Li, J. Wang, W. Zhou, B. Li, C. Huang, P. Li, Z. Guo, W. Tao, Y. Yang, X. Xu, Y. Li, Y. Wang, L. Yang, TCMSP: a database of systems pharmacology for drug discovery from herbal medicines, J. Cheminf. 6 (2014) 13, https://doi.org/10.1186/1758-2946-6-13.
[65] C. Zhao, H. Li, X. Liu, S. Liang, X. Liu, X. Li, Y. Luo, M. Zhu, Dissecting the underlying pharmaceutical mechanism of Danggui Buxue decoction acting on idiopathic pulmonary fibrosis with network pharmacology, Trad Med Res 5 (2020) 178–294, https://doi.org/10.53388/TMR20191102146.
[66] Y. Zhang, L. Gu, J. PuYang, M. Liu, Q. Xia, W. Jiang, M. Cao, Systems bioinformatic approach to determine the pharmacological mechanisms of radix astragali and radix angelicae sinensis in idiopathic pulmonary fibrosis, Phcog. Mag. 17 (2021) 708–718, https://doi.org/10.4103/pm.pm_9_21.
[67] C.T. UniProt, UniProt: the universal protein knowledgebase, Nucleic Acids Res. 45 (2017) D158–D169, https://doi.org/10.1093/nar/gkw1099.
[68] S. Davis, P.S. Meltzer, GEOquery: a bridge between the gene expression Omnibus (GEO) and BioConductor, Bioinformatics 23 (2007) 1846–1847, https://doi.org/10.1093/bioinformatics/btm254.
[69] T. Wu, E. Hu, S. Xu, M. Chen, P. Guo, Z. Dai, T. Feng, L. Zhou, W. Tang, L. Zhan, X. Fu, S. Liu, X. Bo, G. Yu, ClusterProfiler 4.0: a universal enrichment tool for interpreting omics data, Innovation 2 (2021) 100141, https://doi.org/10.1016/j.xinn.2021.100141.
[70] P. Shannon, A. Markiel, O. Ozier, N.S. Baliga, J.T. Wang, D. Ramage, N. Amin, B. Schwikowski, T. Ideker, Cytoscape: a software environment for integrated models of biomolecular interaction networks, Genome Res. 13 (2003) 2498–2504, https://doi.org/10.1101/gr.1239303.

[71] D. Szklarczyk, A.L. Gable, D. Lyon, A. Junge, S. Wyder, J. Huerta-Cepas, M. Simonovic, N.T. Doncheva, J.H. Morris, P. Bork, L.J. Jensen, C.V. Mering, STRING v11: protein-protein association networks with increased coverage, supporting functional discovery in genome-wide experimental datasets, Nucleic Acids Res. 47 (2019) D607–D613, https://doi.org/10.1093/nar/gky1131.

[72] G. Xing, Y. Zhang, X. Wu, H. Wang, Y. Liu, Z. Zhang, M. Hou, H. Hua, Analysis of the efficacy and pharmacological mechanisms of action of zhenren yangzang decoction on ulcerative colitis using Meta-Analysis and network pharmacology, Evid Based Complement Alternat Med 2021 (2021) 4512755, https://doi.org/10.1155/2021/4512755.

[73] P. Gu, D. Wang, J. Zhang, X. Wang, Z. Chen, L. Gu, M. Liu, F. Meng, J. Yang, H. Cai, Y. Xiao, Y. Chen, M. Cao, Protective function of interleukin-22 in pulmonary fibrosis, Clin. Transl. Med. 11 (2021) e509, https://doi.org/10.1002/ctm2.509.

[74] H. Zhang, X. Wang, Y. Shi, M. Liu, Q. Xia, W. Jiang, Y. Zhang, Danggui buxue decoction ameliorates idiopathic pulmonary fibrosis through MicroRNA and messenger RNA regulatory network, Evid Based Complement Alternat Med 2022 (2022) 3439656, https://doi.org/10.1155/2022/3439656.

[75] M.S. Hohmann, D.M. Habiel, A.L. Coelho, W.J. Verri, C.M. Hogaboam, Quercetin enhances ligand-induced apoptosis in senescent idiopathic pulmonary fibrosis fibroblasts and reduces lung fibrosis in vivo, Am. J. Respir. Cell Mol. Biol. 60 (2019) 28–40, https://doi.org/10.1165/rcmb.2017-0289OC.

[76] S.V. Szapiel, N.A. Elson, J.D. Fulmer, G.W. Hunninghake, R.G. Crystal, Bleomycin-induced interstitial pulmonary disease in the nude, athymic mouse, Am. Rev. Respir. Dis. 120 (1979) 893–899, https://doi.org/10.1164/arrd.1979.120.4.893.

[77] T. Ashcroft, J.M. Simpson, V. Timbrell, Simple method of estimating severity of pulmonary fibrosis on a numerical scale, J. Clin. Pathol. 41 (1988) 467–470, https://doi.org/10.1136/jcp.41.4.467.